Glycosyl Inositol Derivatives Related to Inositolphosphoglycan Mediators: Synthesis, Structure, and Biological Activity

Hansjörg Dietrich,[a] Juan Felix Espinosa,[b] José Luis Chiara,[b] Jesús Jimenez-Barbero,[b] Yolanda Leon,[c] Isabel Varela-Nieto,[c] José-Maria Mato,[c] Felix H. Cano,[d] Concepción Foces-Foces,[d] and Manuel Martín-Lomas*[a]

Abstract: Some biologically active structures related to inositolphosphoglycan (IPG) mediators (compounds **3**–**5**) and the corresponding glycosylphosphatidylinositol precursors (compounds **1** and **2**) have been prepared by using an effective synthetic strategy. The basic structural features of these substances have been established by determining the solid-state structure of compound **3**, the solution structure of compounds **3** and **5** using NMR spectroscopy and molecular mechanics calculations, the dynamic properties of trisaccharide **4** using molecular dynamics calculations with explicit water molecules, and the solution structure of **1** and **2** anchored to a detergent micelle. The biological activity of some of these derivatives has also been investigated. It has been confirmed that compound **3** acts as potent mitogen in the chicken's developing inner ear and it has been demonstrated that **3** modulates the expression of Fos which is a molecular marker of cell proliferation.

Keywords: carbohydrates · conformation analysis · glycolipids · inositols · signal transduction

Introduction

The generation of lipid-derived second messengers, such as 1D-*myo*-inositol 1,4,5-trisphosphate, ceramide, diacyl glycerol, and lysophosphatidic acid, after receptor-mediated activation of different lipases has been firmly established in recent years.[1,2] The enzymatic cleavage of uncharacterised glycosyl phosphatidylinositols (GPIs) to produce inositolphosphoglycan (IPG) mediators has been proposed as a new pathway of intracellular signal transduction which has been investigated in the case of insulin and a variety of neurotrophic and growth factors.[3–6] The role of these uncharacterized IPGs as insulin second messengers has been postulated on the basis of their ability to modulate the activity of a number of enzymes, the phosphorylation and dephosphorylation of cellular proteins, protein synthesis and gene expression, lipid metabolism, glucose utilization and the stimulation of cell growth.[4,6–8]

The precise chemical structures of either the IPG mediators or the GPI precursors remain to be elucidated. Two main structural groups of mediators have been proposed on the basis of chemical composition and biological activity: 1) the *c*AMP-dependent protein kinase inhibitors (composed of *myo*-inositol, nonacetylated glucosamine, galactose, and phosphate[9]) and 2) the pyruvate dehydrogenase phosphatase activators (containing *chiro*-inositol, nonacetylated galactosamine, mannose and phosphate[10]). Furthermore, neither the nature of the specific phospholipase involved in GPI hydrolysis nor the mechanism by which this enzyme is regulated are presently known. GPI specific phospholipase C (GPI–PLC) or D (GPI–PLD)[11] activities could be responsible for the release of IPG second messengers, but a detailed study of the specific structural requirements involved in the regulation of GPI cleavage is still lacking. A number of basic chemical and biological aspects of the entire process have, therefore, to be disclosed in order to elucidate the molecular basis of this new receptor-mediated pathway of intracellular signal transduction.

Herein we address some of the above basic chemical aspects as a continuation of our previous studies on the structure of IPG mediators from bovine liver[12] and on the synthesis of glycosyl inositols and oligosaccharides with insulin mimetic activity.[13a–d] We now report an efficient synthesis of some biologically active structures related to

[a] Prof. Dr. M. Martín-Lomas, Dr. H. Dietrich
Grupo de Carbohidratos, Instituto de Investigaciones Químicas, CSIC
Américo Vespucio s/n, Isla de la Cartuja
E-41092 Seville (Spain)
Fax: (+34) 5-4460565
E-mail: mamartin@cica.es

[b] Dr. J.-L. Chiara, Dr. J. Jimenez-Barbero, Dr. J.-F. Espinosa
Instituto de Química Orgánica, CSIC
Juan de la Cierva 3, E-28006 Madrid (Spain)

[c] Prof. Dr. J.-M. Mato, Dr. I. Varela-Nieto, Dr. Y. León, Instituto de Investigaciones Biomédicas, CSIC Arturo Duperier 4, E-28029 Madrid (Spain)

[d] Prof. Dr. F. H. Cano, Prof. Dr. C. Foces-Foces Instituto de Química Fisica Rocasolano, CSIC
Serrano 119, E-28006 Madrid (Spain)

Supporting information for this article is available on the WWW under http://www.wiley-vch.de/home/chemistry/ or from the author.

0947-6539/99/0501-0320 $ 17.50+.50/0

GPIs and GPI hydrolysis, and a detailed conformational study of these structures. Compounds **1**–**4** have been prepared by using a highly effective synthetic strategy.[14] The solid-state structure of **3** has been determined and the solution conformation of **3** and **5** have been established by using molecular mechanics and NMR spectroscopy. Compounds **3** and **5** are expected to be the products generated from **1** after PLC-mediated hydrolysis. The conformation of both **3** and **5** has also been investigated as a function of the pH of the medium. Compound **3** has been previously shown to act as a potent mitogen in the chicken's developing inner ear and different cell types, mimicking the biological activity of natural IPGs.[13b,15] These results have now been confirmed and extended, and show that **3** can modulate the expression of Fos, a molecular marker of cellular proliferation, during the development of the inner ear. Furthermore, the structural and dynamic features of trisaccharide **4**, expected to be released from **2** after PLC-mediated cleavage, has been derived from a molecular dynamics calculation with explicit water molecules. Finally, the solution structure of glycolipids **1** and **2** has also been determined in an aprotic solvent and anchored in a detergent micelle so as to mimic the physiological membrane environment.

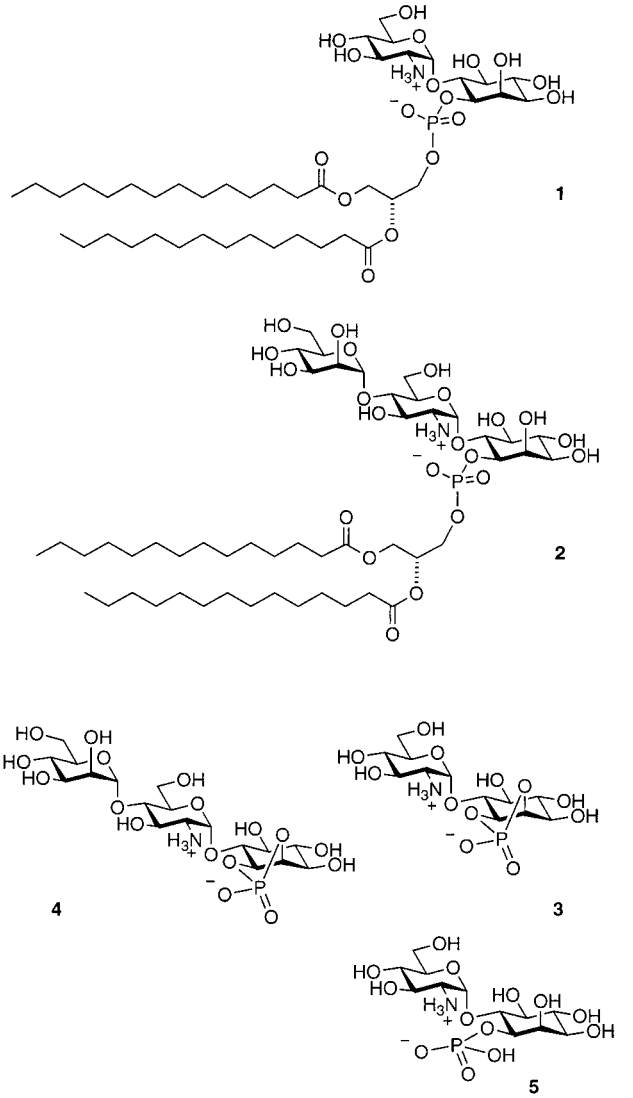

Abstract in Spanish: *Se describe una estrategia sintética para la preparación de una serie de compuestos relacionados con los inositol fosfoglicanos propuestos como segundos mensajeros (compuestos **3**-**5**) y sus correspondientes precursores (glicosil fosfatidilinositoles de tipo **1** y **2**). Se estudian las principales características estructurales de estas sustancias a través de la determinación de la estructura del compuesto **3** en estado sólido, la estructura en solución de los compuestos **3**-**5**- utilizando espectroscopía de RMN y cálculos de mecánica molecular- las propiedades dinámicas del trisacárido **4** - utilizando cálculos de dinámica molecular con moléculas de agua explícitas- y la estructura de los glicolípidos **1** y **2** en solución y en un medio micelar. Se ha investigado también la actividad biológica de estos compuestos y se ha confirmado que el compuesto **3** se comporta como un potente mitógeno en el oído interno del embrión de pollo y que este compuesto modula la expresión del marcador molecular de proliferación FOS.*

Results and Discussion

Synthesis

The synthesis of **1**–**4** involves glycosylation reactions with α-selectivities that, according to experience gained from synthesizing glycosyl inositols,[13a–c] can be achieved by using the trichloroacetimidate glycosylation procedure[16] with 2-azido-2-deoxy sugars as glycosyl donors.[17] These glycosyl donors were prepared as indicated in Scheme 1.

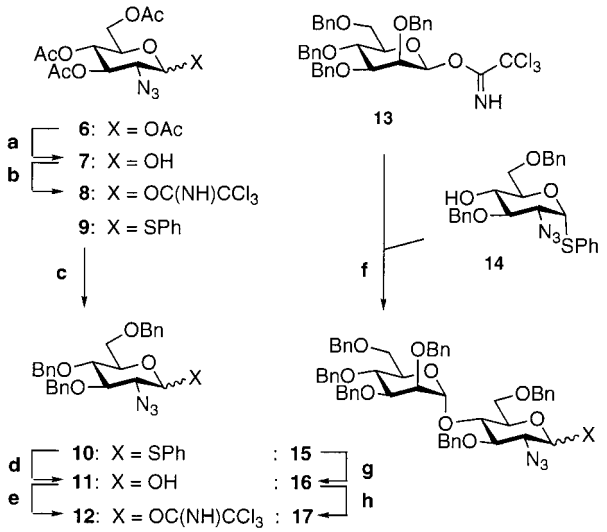

Scheme 1. Reagents: a) $H_2NNH_2 \cdot HOAc$, DMF (92%); b) CCl_3CN, K_2CO_3, CH_2Cl_2 (96%); c) 1. aqueous NaOH, nBu$_4$NHSO$_4$, benzene. 2. BnBr (93%); d) NBS, aqueous acetone (84%); e) CCl_3CN, K_2CO_3, CH_2Cl_2 (92%); f) **12**, TMSOTf, 4 Å molecular sieves, Et_2O (62%); g) NBS, aqueous acetone (88%); h) CCl_3CN, K_2CO_3, CH_2Cl_2 (84%).

The acetylated donor **8**[18] was synthesized from the readily available derivative **6**[19] by selective removal of the 1-*O*-acetyl group[20] and trichloroacetimidate formation under established conditions.[16] The benzylated donor **12**[21] was prepared

from the phenyl thioglucopyranoside **9**, which is readily available from **6**,[22] by one-pot deacetylation and perbenzylation under phase-transfer conditions in excellent yield. Compound **10** was converted into **12** via hemiacetal **11** by treatment with *N*-bromosuccinimide in aqueous acetone[23] and activation with CCl_3CN and K_2CO_3 as a base. The donor **17** was synthesized from the perbenzylated mannopyranosyl trichloroacetimidate **13**[24] and the phenyl thioglycoside derivative **14**, which was obtained from **9** by deacetylation followed by selective di-*O*-benzylation.[22] Reaction of **13** with **14** using trimethylsilyl triflate (TMSOTf) as promoter gave the disaccharide derivative **15** which was then converted into trichloroacetimidate **17** using the sequence outlined for **12**.

Diol **19** was chosen as the *myo*-inositol glycosyl acceptor fulfilling the critical demands of being readily available in optically pure form and of bearing a protecting group pattern fully compatible with the further transformations required (Scheme 2). In addition, as reported for related systems,[25] the expected higher reactivity of the hydroxyl group at C-6 permitted regioselective glycosylation at this position. Furthermore, selective cleavage of the camphor ketal as orthogonal protecting group should also be expected thus allowing phosphorylation of the liberated hydroxyl groups at C-1 and C-2. Therefore diol **19** was synthesized by a modification of a reported procedure (Scheme 2) allowing access to pure product in a multigram scale. Thus, treatment of *myo*-inositol with an excess of L-camphor dimethyl ketal in the presence of H_2SO_4 gave a mixture of *myo*-inositol camphor ketals.[26] Subsequent hydrolysis of the *trans*-ketal functions and *p*-toluensulfonic acid (*p*-TsOH)-mediated equilibration afforded a precipitate consisting of the unprotected *myo*-inositol starting material and a mixture of *cis*-ketals with the desired product **18** as the major component. Ketal **18** was purified by passage of the reaction mixture through a short Florisil column and further crystallization. Regioselective 3,4-bis-protection of **18** was achieved by using 1,3-dichloro-1,1,3,3-tetraisopropyldisiloxane ($TIPIDSCl_2$) as reported previously for its enantiomer.[27]

The key building blocks **24** and **27** (Scheme 3) were prepared as follows. Condensation of trichloroacetimidate **8** with a slight excess of **19** afforded the 6-O-linked α-glycoside **20a** in 80% yield together with a small amount (9%) of the 5-O-linked regioisomer **20b** (see Scheme 2). To fully confirm its regiochemistry by ^1H NMR spectroscopy, compound **20a** was

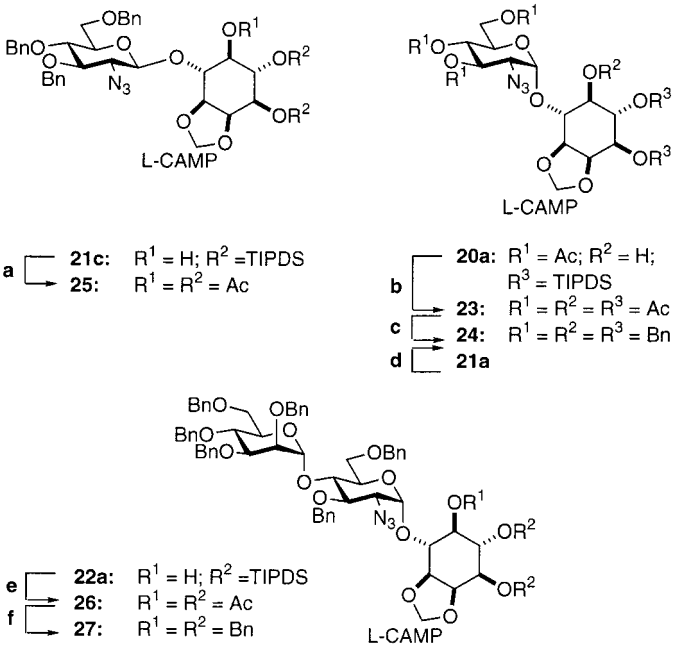

Scheme 3. Reagents: a) 1. Bu_4NF, THF; 2. pyridine, Ac_2O (86%); b) 1. Bu_4NF, THF; 2. pyridine, Ac_2O (quantitative); c) 1. NaOMe, MeOH; 2. BnBr, NaH, DMF (90%); d) 1. Bu_4NF, THF; 2. DMF, NaH, BnBr (72%); e) 1. Bu_4NF, THF; 2. pyridine, Ac_2O (95%); f) 1. NaOMe, MeOH. 2. BnBr, NaH, DMF (90%).

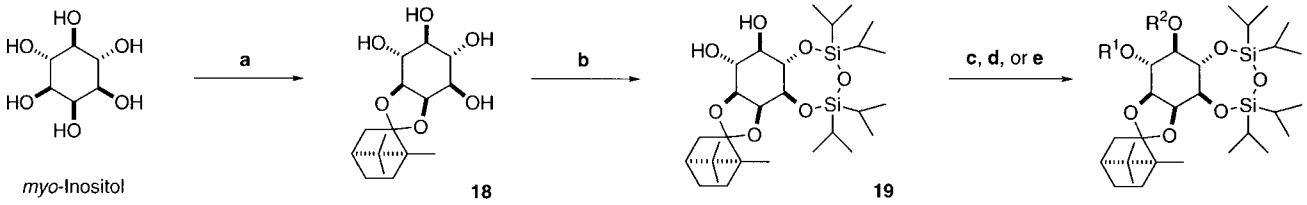

Prod.	20a	20b	21a	21b	21c	22a	22b
R^1	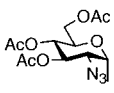	H	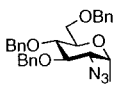	H	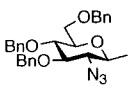	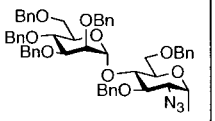	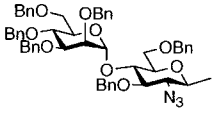
R^2	H	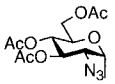	H	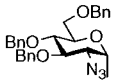	H	H	H
Yield	80%	9%	67%	7%	17%	65%	29%

Scheme 2. Reagents: a) 1. L-camphor dimethyl ketal, H_2SO_4; 2. *p*-TsOH, $CHCl_3$/MeOH/H_2O; 3. crystallization (29%); b) $TIPDSCl_2$, pyridine (93%); c) **7**, TMSOTf, molecular sieves 3 Å, Et_2O; d) **11**, TMSOTf, molecular sieves 3 Å, Et_2O; e) **16**, TMSOTf, molecular sieves 4 Å, Et_2O.

0947-6539/99/0501-0322 $ 17.50+.50/0 *Chem. Eur. J.* **1999**, *5*, No. 1

transformed into **23** by desilylation followed by acetylation (Scheme 3). Deacetylation and benzylation afforded **24** ready for the final transformations. This route to **24** was preferred to the alternative approach starting from the more reactive trichloroacetimidate **12**, since glycosylation of **19** with this donor at $-40\,^{\circ}C$ using TMSOTf as promoter afforded the α-linked 6-*O*-glycoside **21a** in only 67% yield together with the regioisomer **21b** (7%) and the β-linked 6-*O*-glycoside **21c** (17%). All attempts to improve the regio- and the stereoselectivity of the reaction by decreasing the reaction temperature[16] had no significant effect on product distribution. Desilylation of **21a** followed by benzylation yielded again **24**. The former route to **24** was therefore more efficient affording this key ketal in 64% overall yield after five steps from the common precursor **6** in contrast to the 28% overall yield obtained and the six steps required in the latter route. Compound **27** was synthesized from trichloroacetimidate **17** and diol **19**. This reaction gave a 2.2:1 α/β mixture of glycosides from which **22a** was easily separated. Again, to ease characterization, this product was desilylated and subsequently acetylated to give **26**. Deacetylation and benzylation afforded **27**, ready for the final transformations. The regio- and stereochemistry of all glycosylation products was unambiguously derived from $^1H-^1H$ COSY and proton-decoupled NMR spectra of the acetylated intermediates **23**, **25**, and **26**.

For the synthesis of cyclic phosphate **3**, ketal **24** was treated with trifluoroacetic acid to give diol **28** (Scheme 4). Reaction

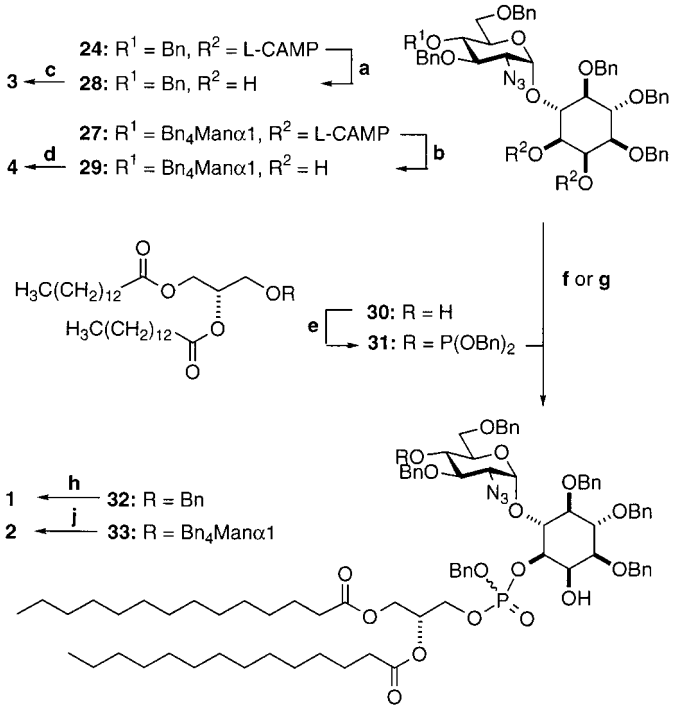

Scheme 4. Reagents: a) aqueous $CHCl_3$, TFA (84%); b) aqueous $CHCl_3$, TFA (88%); c) 1. $MeOP(O)Cl_2$, pyridine; 2. Pd/C, H_2, NH_4OAc, THF/EtOH/H_2O. 3. 1X-200 (HCO_3^-) (62%); d) 1. $MeOP(O)Cl_2$, pyridine; 2. Pd/C, H_2, NH_4OAc, THF/EtOH/H_2O; 3. TMD-8 (H^+/OH^-) (90%); e) $(BnO)_2PNiPr_2$, tetrazole (92%); f) **27**, pyridine·HBr_3, CH_2Cl_2/pyridine (54%, +22% recovered **27**); g) **28**, pyridine·HBr_3, CH_2Cl_2/pyridine (28%, +22% recovered **28**); h) Pd/C, H_2, EtOAc/THF/EtOH/H_2O (quantitative); j) Pd/C, H_2, EtOAc/THF/EtOH/H_2O (61%).

of **28** with *N*-methylpyridinium phosphodichloridate[28] followed by hydrogenolytic debenzylation and concomitant azide reduction in buffered medium afforded **3** in 62% yield after purification by ion exchange chromatography. Compound **4** was similarly synthesized from **27**. This synthetic strategy considerably improves procedures previously reported for the preparation of **3**.[13b,29]

Finally, the GPI substructures **1** and **2** were prepared from precursors **28** and **29**, respectively, by regioselective phosphorylation using the phosphite-phosphonium salt methodology.[30] Dimiristoylglycerol phosphite (**31**) was obtained from dimiristoylglycerol (**30**) by reaction with dibenzyl *N*,*N*-diisopropylphosphoramidite and 1*H*-tetrazol as proton source.[31] Reaction of **28** with phosphite **31** in the presence of pyridinium bromide perbromide (PBP) and pyridine afforded **32** in 74% yield. Glycolipid **33** was similarly obtained from diol **29**. Hydrogenolitic cleavage of benzyl groups with concomitant reduction of the azido group yielded target compounds **1** and **2**.

Biological activity

Cyclic phosphate **3** stimulated proliferative growth in the otic vesicle. The effects of **3** have been studied on stage 18 otic vesicles that were isolated and cultured for 24 h. A typical experiment is shown in Figure 1 top in which the effect of **3** at concentrations of 1 and 10 μM is compared with otic vesicles grown in parallel without additions (0S) or in the presence of 1 nM insulin-like growth factor I (IGF-I). Otic vesicles incubated with **3** acquired a morphology that corresponded to stage 19^+ otic vesicles developed in vivo. The rate of DNA synthesis was estimated in parallel experiments by measuring [^{3}H]thymidine incorporation into acid precipitable material (Figure 1 bottom). Compound **3** induced [^{3}H]thymidine uptake in a concentration-dependent manner with a maximal effect at a concentration of 10 μM.

Compound **3** also modulates Fos levels in the otic vesicle, and Figure 2 shows a Western blot analysis of otic vesicles stimulated with **3** at different times. Fos induction by **3** was transient and reached a peak after two hours (see lanes labeled sense in Figure 2). Densitometrical estimates of stimulation at $t = 2$ h gave a 2.2 ± 0.2-fold increase above the control value ($n = 3$). As with serum or growth factors, after 24h the amount of Fos protein was variable.[32] *c-Fos* antisense oligonucleotides inhibited the effect of **3** (lane labeled antisense in Figure 2), while random oligonucleotides had no effect on the stimulation (lane labeled random in Figure 2). Several simple carbohydrates (glucosamine, galactose, inositol) were used as controls and none of them stimulated cellular proliferation or Fos expression.

In conclusion, the above results demonstrate that **3** is a potent growth stimulator in the otic vesicle and induces Fos expression. Furthermore, *c-fos* antisense nucleotides inhibit the effects of **3**. Fos is developmentally regulated during the proliferative period of otic vesicle development and it is an essential element in propagating mitogenic signals.[32,33] IGF-I induces Fos expression and *c-fos* antisense nucleotides inhibit IGF-I with the GPI/IPG signalling system being upstream of

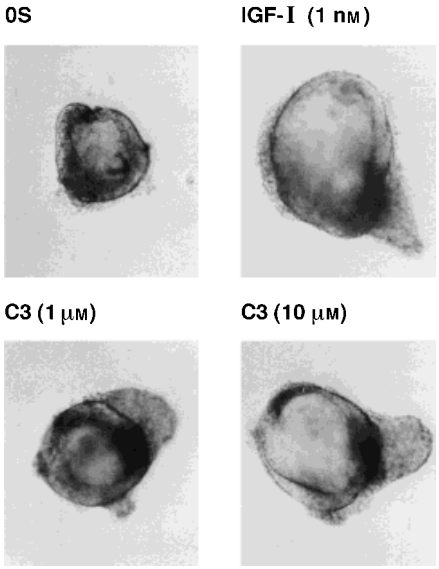

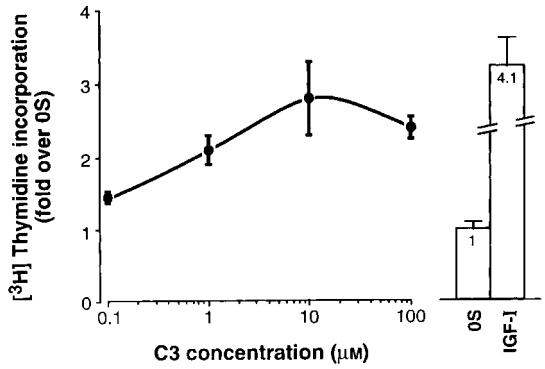

Figure 1. Effect of compound **3** on otic vesicle growth. Top: Microphotographs of a typical otic vesicle culture. Fresh otic vesicles obtained from stage 18 chicken embryos were arrested by culture in serum-free medium 199 and then were stimulated for 24 h by addition of insulin-like growth factor (IGF-I), compound **3** at the doses indicated in brackets, or without additions (0S). Bottom: Acid-precipitable [^{3}H]thymidine incorporation was measured in otic vesicles cultured in the presence of increasing concentrations of **3** from 0.1 to 100 μM. Data are representative of at least three different experiments with an average of four otic vesicles per condition. The bars to the right indicate [^{3}H]thymidine uptake in otic vesicles cultured in serum-free medium (0S) or 1 nM IGF-I for 24 h.

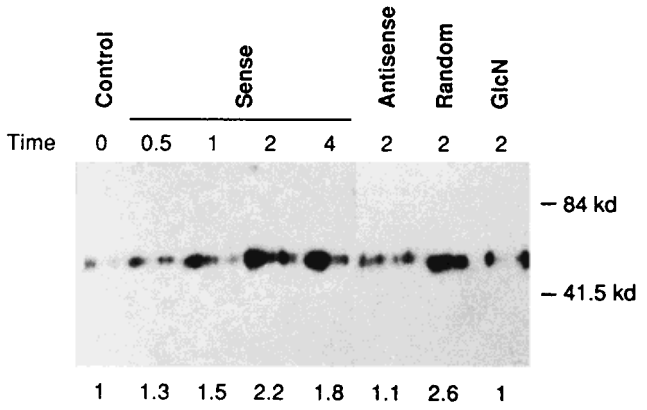

Figure 2. Time-course of stimulation of Fos oncoprotein expression by **3**. Western blotting analysis of stage 18 otic vesicles stimulated with 1 μM **3** in the presence of sense, antisense, or random AUG-c-*fos* oligonucleotides for the periods of time indicated. Control represents levels of Fos at time 0. Lane labelled GlcN indicates levels of Fos in parallel otic vesicles cultured in the presence of 1 μM glucosamine. The resulting autoradiogram was quantitated and data are expressed as fold change in Fos protein over the control value which was set at 1.

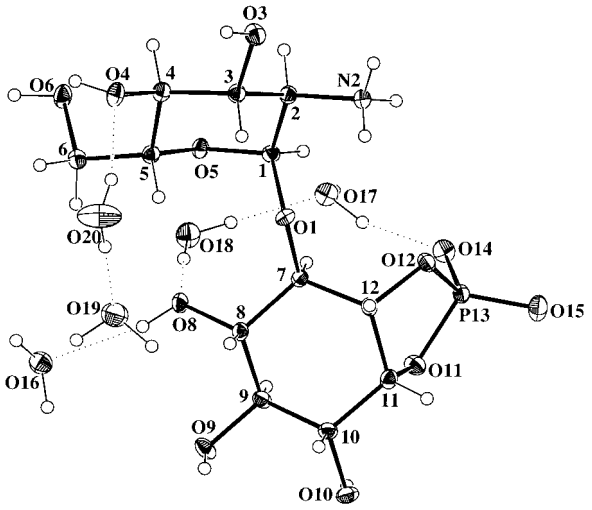

Figure 3. A perspective view of the asymmetric unit of **3** showing the numbering system. Non-hydrogen atoms are represented by displacement ellipsoids at 30% probability level. Dotted lines indicate bonds.

Fos for the propagation of the IGF-I signal.[33] The effects of **3** indicate that this compound is able to mimic IGF-I effects in the otic vesicle.

Structure

The crystal structure of compound **3** was determined by X-ray analysis at 250 K (Figure 3). Selected geometric parameters are reported in Table 1. The molecule appears as a zwitterion with the positive charge on N-2′ and the negative charge delocalized between O-14 and O-15. The molecular structure shows bond lengths and angles comparable with the average values found for related inositol derivatives, cyclic phosphate rings, and glucosamine derivatives carrying the NH_3^+ group (29, 2, and 7 structures, respectively, retrieved from the Cambridge Data Base).[35] The N–C distance is 1.493(4) Å, which agrees with the average value 1.497(12) Å found for similar glucosamine derivatives with a NH_3^+ group (7 structures), but it is significantly longer than the average value of 1.458(11) Å obtained from 11 glucosamine structures with neutral C-NHR groups. The P atom resides in an approximate tetrahedral environment. The two pairs of P–O bonds (endocyclic and exocyclic bonds) have lengths close to the values for the two reference structures (CYCYPH10 and CY9CYP20; CSD refcodes). The endocyclic O-5′–C-5′ and O-5′–C-1′ bond lengths (Table 1) are significantly different as a consequence of the anomeric effect. The pyranose and inositol rings adopt chair conformations [Cremer and Pople parameters:[36] $q_2 = 0.054(3)/0.103(3)$, $q_3 = 0.513(3)/0.523(3)$ Å, $\theta_2 = 5.2(3)/11.1(3)^\circ$ vs $q_2 = \theta_2 = 0$ for the ideal conformation]. The inositol ring appears slightly flattened due to the fused cyclic phosphate five-membered ring which

0947-6539/99/0501-0324 $ 17.50+.50/0 *Chem. Eur. J.* **1999**, *5*, No. 1

Table 1. Selected geometrical parameters [Å, °] for the X-ray structure of **3**.

C1 – O5	1.406(4)	C5 – O5	1.442(3)
O11 – P13	1.615(2)	O12 – P13	1.609(2)
O14 – P13	1.490(2)	O15 – P13	1.483(2)
O11-P13-O12	96.9(1)	O14-P13-O15	116.1(1)
O1-C7-C8-C9	– 172.7(2)	C12-C7-C8-C9	– 55.4(3)
O8-C8-C9-C10	177.6(2)	C7-C8-C9-C10	59.5(3)
O9-C9-C10-C11	– 177.9(2)	C8-C9-C10-C11	– 55.6(3)
O10-C10-C11-C12	173.8(2)	C9-C10-C11-C12	47.4(3)
O11-C11-C12-C7	76.9(3)	C10-C11-C12-C7	41.1(3)
O12-C12-C7-C8	– 75.3(3)	C11-C12-C7-C8	48.4(3)
O3-C3-C4-C5	175.4(2)	C2-C3-C4-C5	56.2(3)
O4-C4-C5-O5	178.8(2)	O4-C4-C5-O5	– 61.4(3)
C6-C5-O5-C1	– 171.0(2)	C4-C5-O5-C1	65.7(3)
O1-C1-C2-C3	– 67.7(3)	O5-C1-C2-C3	– 61.5(3)
N2-C2-C3-C4	– 177.6(2)	C1-C2-C3-C4	54.7(3)

Hydrogen interactions	X – H	H ··· X	X ··· Y	X – H ··· Y
N2-H21 ··· O6 (1 – *x*,1/2 + *y*,3/2 – *z*)	0.99(5)	1.80(6)	2.753(4)	176(4)
N2-H22 ··· O18 (1 – *x*,1/2 + *y*,3/2 – *z*)	0.99(5)	2.13(5)	2.949(4)	177(4)
N2-H23 ··· O10 (1/2 – *x*,2 – *y*, – 1/2 + *z*)	0.99(5)	1.98(6)	2.8834)	163(5)
O3-H30 ··· O14 (*x*,*y*, – 1 + *z*)	0.98(5)	1.84(6)	2.714(3)	154(5)
O4-H40 ··· O16 (1/2 – *x*,1 – *y*, – 1/2 + *z*)	1.03(5)	2.03(6)	2.870(3)	175(4)
O6-H60 ··· O9 (1/2 – *x*,1 – *y*, – 1/2 + *z*)	0.99(5)	1.72(6)	2.629(3)	170(5)
O8-H80 ··· O16	0.92(5)	2.03(5)	2.877(3)	161(4)
O9-H90 ··· O17 (– 1/2 + *x*,3/2 – *y*,2 – *z*)	0.98(5)	1.92(5)	2.713(3)	169(5)
O10-H100 ··· O20 (*x*,*y*,1 + *z*)	0.86(5)	1.83(5)	2.684(4)	175(4)
O16-H161 ··· O18 (1/2 – *x*,1 – *y*, – 1/2 + *z*)	0.84(7)	2.15(7)	2.975(4)	170(5)
O16-H162 ··· O14 (– 1/2 + *x*,3/2 – *y*,2 – *z*)	0.89(6)	2.03(6)	2.913(3)	168(5)
O17-H171 ··· O14 (1 – *x*, – 1/2 + *y*,5/2 – *z*	0.92(5)	1.84(5)	2.733(3)	162(4)
O17-H172 ··· O15	0.82(5)	1.89(5)	2.700(3)	169(4)
O18-H181 ··· O8	0.88(5)	2.00(5)	2.881(3)	173(4)
O18-H182 ··· O17	0.84(5)	1.94(5)	2.775(3)	172(4)
O19-H191 ··· O15(1/2 – *x*,2 – *y*, – 1/2 + *z*)	0.96(7)	1.78(7)	2.748(4)	177(5)
O19-H192 ··· O3)(– 1/2 + *x*,3/2 – *y*,1 – *z*)	0.87(6)	1.98(6)	2.830(4)	165(5)
O20-H201 ··· O4	0.82(6)	2.11(6)	2.901(4)	163(5)
O20-H202 ··· O19	0.86(6)	1.84(6)	2.705(4)	177(5)

presents a distorted envelope conformation flapping at C-7 [$q_2 = 0.391(2)$ Å, $\varphi_2 = 103.9(3)^\circ$ vs $\varphi_2 = 108^\circ$ or 90° for the ideal envelope or twist conformation, respectively]. All substituents at the inositol ring with the exception of O-14 and, to some extent, O-15 are purely equatorial as confirmed by the configurational angles.[37] The crystal packing is provided by a dense network of hydrogen bonds involving the NH_3^+ and OH groups and water molecules (Table 1). All the water molecules and the hydroxyl groups act as both donors and acceptors of hydrogen bonds

Conformational studies in water solution

Few conformational studies of GPI-related inositol-containing oligosaccharides have been published to date.[38] The study of a phospolipid from Leishmania major allowed one to conclude that major oscillations occurred around the glycosidic linkages of the molecule. Nevertheless, in this example, the induced significant torsional variations may be due to the presence of two phosphodiester linkages in the structure.[38]

The structures of cyclic phosphate **3** and phosphate **5**[13a,c] in solution have been investigated by NMR spectroscopy and molecular mechanics calculations.[39] The presence of the acetal group, and therefore, the anomeric and exo-anomeric effects[40] pose a problem for devising a force field for sugars, although a number of them are now available.[41] The AMBER force field[42] was chosen in this case, since it has been modified to deal with oligosaccharides[43] and, in addition, it provides adequate parameters for phosphate groups. Nevertheless, in order to be rigourous enough, different torsional variables have to be considered for a detailed conformational analysis. Besides the glycosidic torsion angles, defined in this case as Φ H1′-C1′-O1′-C6 and Ψ C1′-O1′-C6-H6, the different possible orientations of the phosphate group were also condidered. In this context, the analysis of eighteen relaxed energy maps (see Supporting Information) calculated with AMBER for **3** and **5** indicated that the shape of the surfaces depends on the initial conformation of the phosphate group and illustrates the importance of considering all staggered conformations around the C1–O1 and O1–P linkages as well as the c (clockwise) and r (anticlockwise) orientation of the secondary hydroxyl groups. The adiabatic surfaces built from the relaxed maps are shown in Figures 4 and 5 along with the corresponding probability distribution maps. For **3**, about 11 % of the surface is populated, and two local minima, A and B, are predicted. Approximately 94 % of the population is concentrated in a central region around global minimum A, defined by values of Ψ between -120° and 60° and Φ between -80° and 0°. In addition, 6 % of the population is located around minimum B. On the other hand, for the noncyclic phosphate **5**, about 8 % of the total surface is populated, and 90 % of the population concentrated around global minimum A. In this case, Ψ angles rank between -75° and 60° and Φ angles between -80° and 0° (Table 2 and Figure 5). About 4 % of the population appears in this case t be concentrated around minimum B. The AMBER calculations predict, therefore, a somehow greater flexibility around

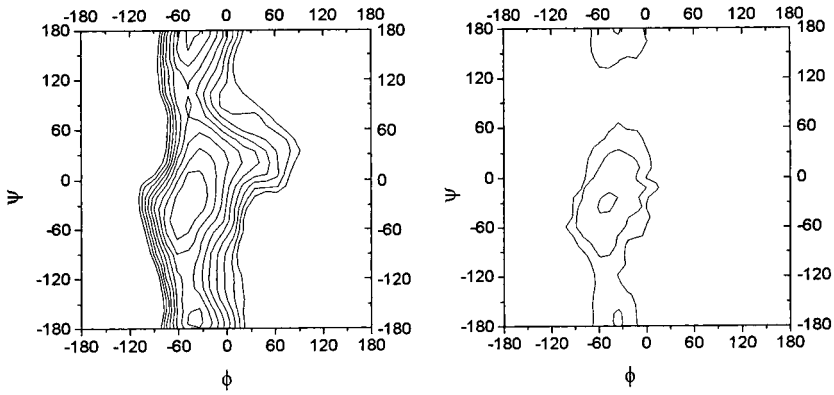

Figure 4. Relaxed adiabatic energy map (left column) calculated by using AMBER ($\varepsilon = 80$) for compound **5**. The level contours are given every kcal mol^{-1}. The probability distribution plot of conformers is also given (right column). The contours are drawn at 10 %, 1 %, and 0.1 % probability levels.

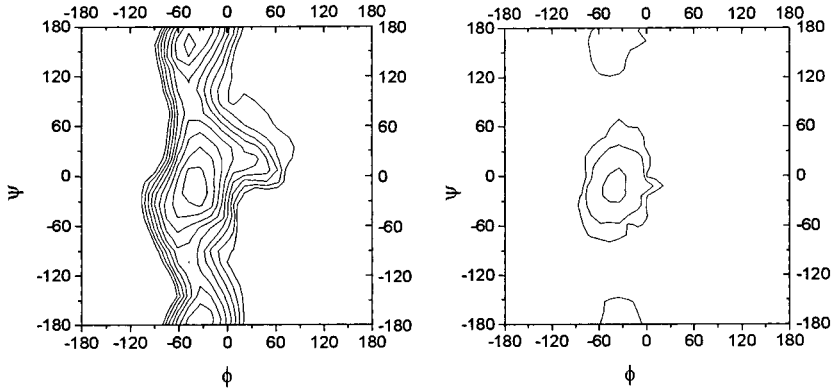

Figure 5. Relaxed adiabatic energy maps (left column) calculated by using AMBER ($\varepsilon = 80$) for compound **3**. The level contours are given every kcal mol^{-1}. The probability distribution plot of conformers is also given (right column). The contours are drawn at 10%, 1%, and 0.1% probability levels.

Table 2. Torsion angles for the local minima of **5** and **3** and X-ray structure of **3**.

	5		**3**		
	AMBER		AMBER		X-ray
Torsion	Minimum A	Minimum B	Minimum A	Minimum B	
Φ	−38.1	−50.2	−46.4	−40.7	−37.2
Ψ	−17.5	156.0	−22.4	−165.2	10.9

the glycosidic bond of the cyclic phosphate, **3**. A view of the global minima for each compound is shown in Figure 6 top and 6 bottom

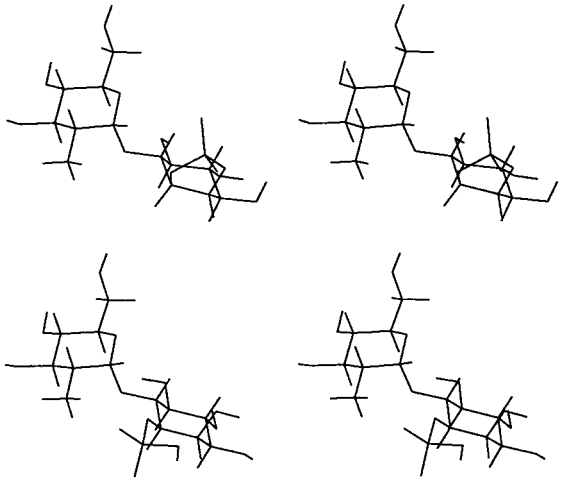

Figure 6. Stereoview of the AMBER global minimum of compound **3** (top) and compound **5** (bottom).

The above predictions have been experimentally tested by NMR spectroscopy.[44] ^{1}H NMR chemical shifts are included in the Supporting Information. Figure 7 shows a superposition of the key interresidue proton–proton distances on the probability distribution map plots for compounds **3** and **5**. The exclusive NOEs[45] that unequivocally characterize the A and B energy minima are H1′–H6 and H1′–H5, respectively. Therefore, the observed NOE values will be sensitive to the actual population of each conformer. The existence of strong NOE between H1′ and H6 and not between H1′ and H5 indicates that the region corresponding to minimum A is heavily populated in both compounds **3** and **5**. The presence of minimum B cannot be experimentally demonstrated in either substance, indicating a maximum population of this minimum of 5% (corresponding to the estimated limit of detection of NOEs). Nevertheless, there is a structural characteristic which differentiates **3** from **5**. The NOE between H1 and H1′ protons is present in the NOESY spectrum of **3.** On the other hand, this enhancement is absent in that of **5**.

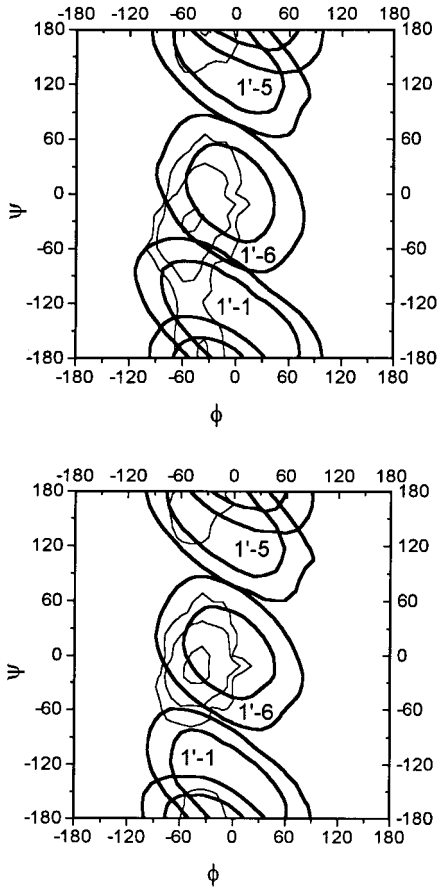

Figure 7. Superimposition of the key NOEs predicted for compound **3** (top) and compound **5** (bottom) on the conformational probability distribution plots. The contours are drawn at 10%, 1%, and 0.1% probability levels. Key NOEs are also indicated.

According to Figure 7, the H1–H1′ distance intersects with the populated area corresponding to the central energy region in Figure 7 bottom, but does not overlap with any populated region in Figure 7 top. Thus, this H1–H1′ distance is indicative of a higher flexibility around the glycosidic linkages of the cyclic phosphate **3** in comparison to those of **5**, as predicted by the AMBER calculations. A semiquantitative treatment of the NOE data according to a full relaxation matrix analysis[46]

0947-6539/99/0501-0326 $ 17.50+.50/0 *Chem. Eur. J.* **1999**, *5*, No. 1

Table 3. Experimental and calculated normalized 1D-NOESY intensities [%] for **5** and **3** in D_2O at 30°.

	Mixing time [ms]	250		400		600		800	
	Proton Pair	Exp.	Calcd.	Exp.	Calcd.	Exp.	Calcd.		
5	H1′/H6	3.6	3.5	5.1	5.6	–	–	–	–
	H1′/H1	not observed	< 1%	not observed	< 1%	–	–	–	–
3	H1′/H6	–	–	5.3	5.1	7.8	7.6	10.7	10.0
	H1′/H1	–	–	1.5	1.7	2.0	2.6	2.3	3.3

(see Experimental Section) was also performed. The agreement between calculated and observed NOEs was excellent (Table 3). Therefore, it can be concluded that the three-dimensional structures of these two compounds may be described by a major conformer A, which undergoes torsional oscillations around the regions defined in Figure 4 and 7. It is noteworthy to mention that for the acyclic compound **5**, both amino and phosphate charged groups are fairly close in space in minimum A, and that, therefore, their mutual interaction could have a relevant structural influence.

Thus, in a further step, the ^{31}P and ^{1}H NMR spectra of compounds **3** and **5** were also analyzed as a function of pH. These data provided relevant information regarding the influence of the ionization state of the amino and phosphate groups on the distinct conformational behavior of these two molecules (Figure 8left and 8right). Monotonical upfield shifting of the H2′ signal—the proton on the carbon bearing the NH_2 group—in the ^{1}H NMR spectrum, accompanied by downfield shifting of the phosphorus signal in the corresponding ^{31}P NMR spectra, was observed with increase in pH. For phosphate **5**, the observed inflection of the ^{31}P titration curve corresponded to a small change of the H2′ curve. In addition, the observed inflection of the H2′ titration curve was linked to a small change of the ^{31}P curve. On the other hand, a markedly different behavior was observed for cyclic phosphate **3**, where both charged groups are close in space. The pK_a value of the phosphate group of **5** (5.5) was similar to that expected for a phosphoric acid monoester. However, that of the amino group (10.3) was much higher than those reported for amino acids and also higher than the value found for the cyclic phosphate analogue, **3** (8.0). These experimental observations unequivocally reflect the existence of a through-space interaction between the amino and phosphate groups in compound **5** that could restrict the mobility around the $\alpha 1-6$ linkage, as has been deduced above. Furthermore, since the conformational behavior of **5** could be sensitive to pH, NOESY spectra were measured at pH 5, 7, and 11. The ratio between the key interresidue NOE H1′–H6 and H1′–H2′ (Table 4) is considerably increased at pH 11, thus indicating a closer proximity of H1′ and H6 in these conditions. According to the conformational map (see Figure 7), this fact is an indication of a decrease of Ψ angle and, consequently, an increase of the

Table 4. Ratio of key inter/intraresidue H1′-H6/H1′-H2′ NOEs as a function of pH for **5** from NOESY experiments (mixing time = 700 ms) at 30° C.

pH	5	7	11
ratio	1.3	1.6	5.7

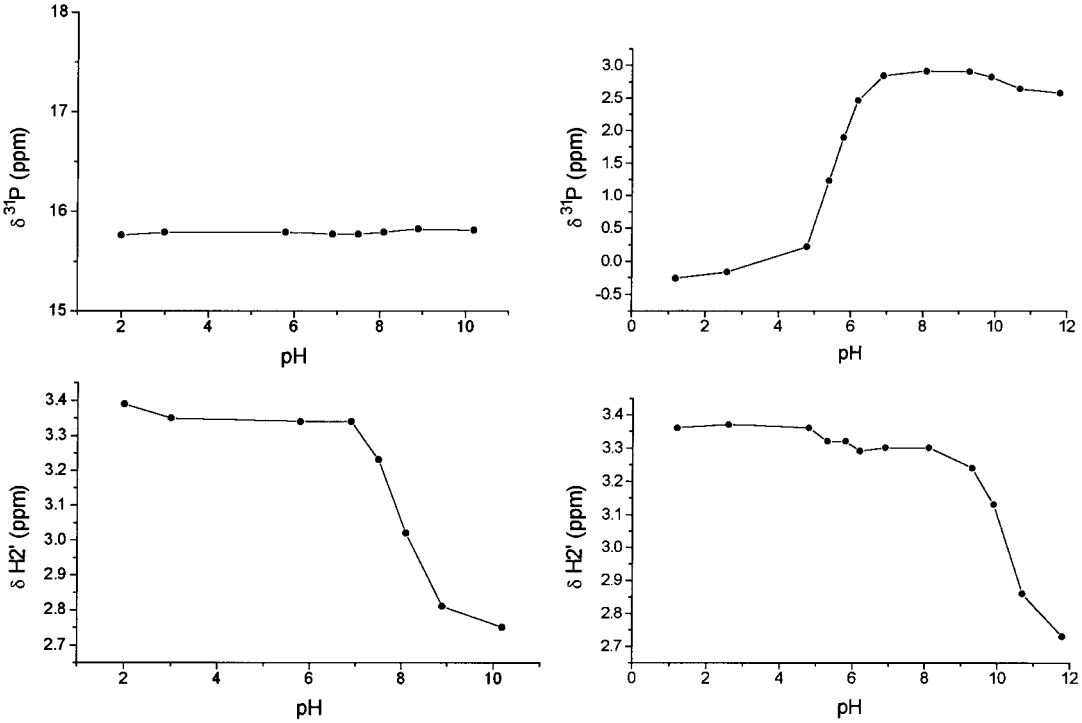

Figure 8. The pH titration curves for compound **3** (left) and compound **5** (right), showing the behavior of ^{31}P and ^{1}H chemical shifts.

distance between the phosphate and the amino group, as expected at higher pH, where the amino group is not charged.

Next, the solution conformation of **4** was also investigated, since it is relevant to most of the GPI anchors reported to date. Besides, it may help to define the influence of an additional pyranoid moiety in the global conformational and dynamical behavior of the molecule.[47] A relaxed map for the substructure Manα1–6GlcNH$_2$ was built which showed that 11% of the surface was populated (Figure 9). Although two minima were predicted by AMBER, again only the global minimum could be experimentally detected. The existence of a strong interresidue NOE between H1 and H4′ (Table 3 and 5) indicated that the region around the global minimum is heavily populated. With regard to the GlcNH$_2$$\alpha$1–6*myo*-inositol moiety, the NOE between H1′ and H6 was observed, as well as a small one between H1 and H1′, which was also present in the isolated disaccharide entity (see above).

Table 5. Experimental 1D-NOESY and 2D-ROESY itensities [%] or **4** in D_2O at 30°.

	NOESY		ROESY	
Proton pairs	300 ms	400 ms	150 ms	300 ms
H1′/H6	3.4	6.2	not determined	9.8
H1″/H4′	2.0	2.6	2.9	5.3
H1′/H1	0.8	1.2	1.0	1.8

In order to evaluate the dynamical behavior of this molecule, molecular dynamics simulations in the presence of explicit water molecules were carried out.[48] A 400 ps simulation was performed in the presence of 233 explicit water molecules by using the AMBER force field. The results obtained are very similar to those obtained by the much less time-consuming molecular mechanics protocol described above (Figure 10). The glycosidic torsion angles cover a well defined region of the Φ/Ψ map. For the Manα1–6GlcNH$_2$ linkage, oscillations between $-80°$ and 0° and between $-60°$ and 40° were observed for Φ and Ψ, respectively. With regard to the GlcNH$_2$$\alpha$1–6*myo*-inositol linkage the range was smaller, between 90° and $-40°$ for Φ and between $-80°$ and $-10°$ for Ψ. Thus, this part of the molecule seems to be more constrained. In order to gain more information on the time scale and nature of the motions around the glycosidic linkages,[49] internal motion correlation functions were calculated for the key interresidue proton–proton vectors of the molecule.[50] Thus, both interresidue H1′–H6 and H1–H4′ distances, as well as the intraresidue H1′–H2′ vector were chosen. The calculations were performed using a molecular fixed coordinate frame through which global reorientation was removed.[51] Five different parts

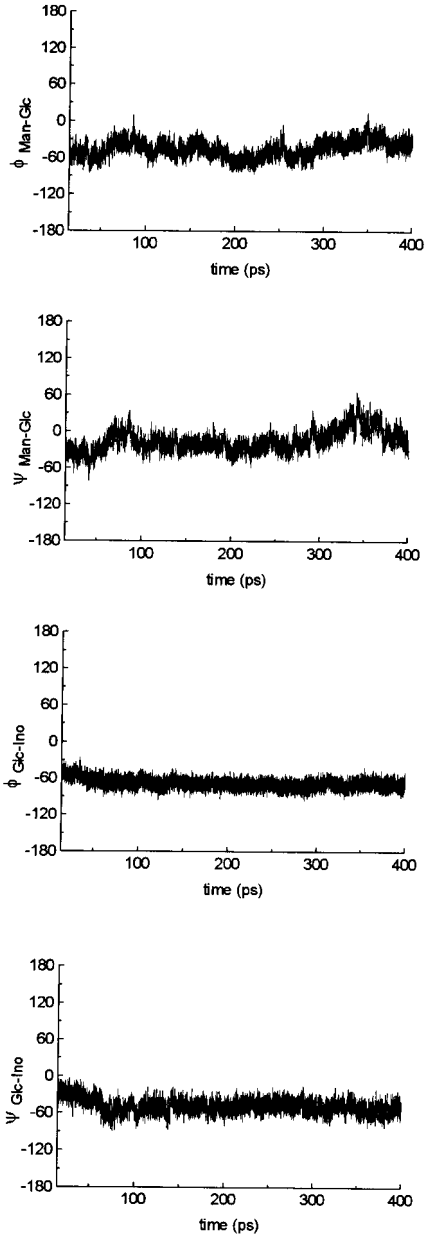

Figure 10. Trajectory plots of the MD simulation (400 ps) of compund **4** in a box of water molecules. The trajectories of the simulation for Φ and Ψ coordinates for every glycosidic linkage are shown.

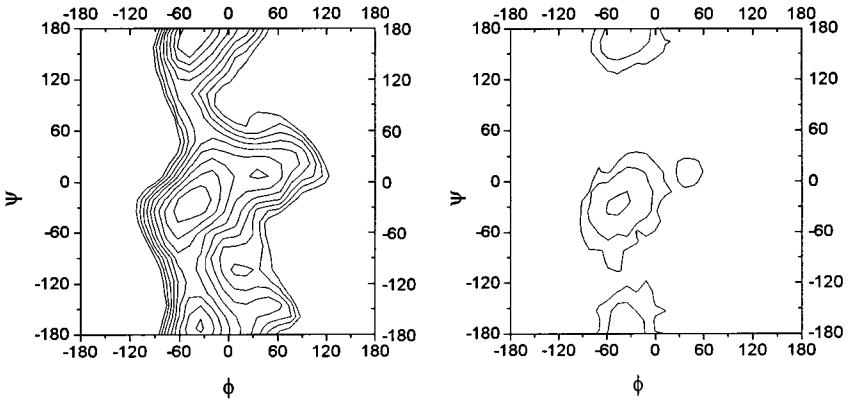

Figure 9. Relaxed energy map (left column) calculated by using AMBER ($\varepsilon = 80$) for the Manα1–6GlcNH$_2$ linkage of compound **4**. The level contours are given every kcal mol^{-1}. The probability distribution plot of conformers is also given (right column). The contours are drawn at 10%, 1%, and 0.1% probability levels.

0947-6539/99/0501-0328 $ 17.50+.50/0 *Chem. Eur. J.* **1999**, *5*, No. 1

of trajectories, with no major transitions of the glycosidic linkages, were chosen to calculate the internal motion correlation functions. The fast internal motions were satisfactorily sampled and the corresponding plateau (see Supporting Information) was reached after a few picoseconds. The correlation functions were used to derive generalized order parameters using the Lipari and Szabo formalism.[52] The results (summarised in Table 6) unequivocally indicated that

Table 6. Generalized order parameters (S^2) calculated from the internal motion correlation functions of different portions of MD trajectory of compound **4** in explicit water.

	Trajectory					
Proton Pair	A	B	C	D	E	Average
H1′/H2′	0.92	0.85	0.82	0.94	0.95	0.90
H1′/H6	0.83	0.74	0.60[a]	0.90	0.91	0.84
H1/H4	0.75	0.65	0.78	0.76	0.80	0.75

[a] This value was excluded since the corresponding plateau was not reached.

there exists a higher restriction around the $GlcNH_2\alpha1-6$*myo*-inositol linkage than around the $Man\alpha1-4GlcNH_2$ bond, since the corresponding order parameters differ in about 0.1 units (0.84 and 0.75, respectively). For comparative purposes, the order parameter of the intraresidue H-1′/H-2′ vector was calculated to be 0.90 units. Thus, according to the calculations, it can be stated that the torsional oscillations around the $GlcNH_2\alpha1-6$*myo*-inositol glycosidic linkage are rather constrained to a limited region of the potential energy surface. The $Man\alpha1-4GlcNH_2$ part is less constrained and may undergo more important torsional oscillations. In all cases, the time scale of the internal motions is in the range of a few tens of ps, which are probably related to librations of the pyranoid rings and to oscillations within the energy wells around the global minima.[53] Thus, from the global consideration of the data obtained, a satisfactory agreement between observed and computed parameters may be deduced. The conformation of the trisaccharide entity may be well described by the average structure depicted in Figure 11.

In nature, these structures are covalently anchored to diacylglycerol moieties, and therefore, their mode of presentation and/or conformational behavior could vary depending on the environment. Thus, and finally, the three-dimensional structure of glycolipids **1** and **2** was also investigated by using NMR spectroscopy (see Supporting Information). Two approaches were used as explained below.

First, NOE experiments, under different experimental conditions were recorded in $DMSO-D_2O$ solutions.[54] This solvent mixture was used to increase the solubility of the molecule and to detect clear NOEs. Different conditions were considered to perform the NOE experiments and to minimize the influence of a *wrong* correlation time.[55] Thus, selective 1D-NOESY, 1D-ROESY, and 1D-T-ROESY experiments were carried out. In all cases, the results obtained were very similar (Figure 12). In fact, for compound **1**, only the above-mentioned interresidue H1′–H6 NOE was observed, again indicating that the only conformation around the glycosidic linkage which is experimentally observable (therefore, present in more than 90%) is that defined by the region around global minimum A (see above for compounds **3** and **5**). Thus, according to these data neither the solvent nor the presence of the diacylglycerol moiety apparently affect the conformational behavior around the glycosidic linkages.

Second, in order to try to mimic the natural environment in which the glycolipids exist, NMR spectra were recorded for aqueous solutions of **1** in the presence of perdeuterated SDS micelles.[56] The NOEs under regular conditions (1D-NOESY) were now strong and negative, indicating the existence of large correlation times for the corresponding proton–proton vectors. This fact is an indication of the integration of the glycolipid in the SDS micelle, with the corresponding increase of the molecular size and, thus, effective correlation time. Again, only the interresidue H1′–H6 NOE was detected, indicating similar conformational behavior for the glycosidic linkage in this environment compared to $DMSO-D_2O$. Only a minor difference was observed: in contrast with the results in $DMSO-D_2O$ solution, the observed NOE between H1′ and H2′ became stronger than that between H1′ and H6 (Figure 12 right) under the different experimental (either longitudinal or transversal) conditions.[57] This fact probably indicates that different average interresidue distances occur in the two media; the distance in SDS is somehow higher than that in the solvent mixture. From the structural point of view, this fact can be correlated with a minor shifting of the population distribution, always within the region defined by minimum A. The existence of major conformational variations between both environments may be discarded as well as the presence of a significant influence of the lipid chain on the glycosidic torsions. Therefore, the sugar moieties are oriented outside the micelle, and do not present any interaction with it.

Finally, the ^1H NMR spectrum of glycolipid **2** was assigned through a combination of regular correlated spectroscopy and HSMQC techniques (chemical shift data are given in the supporting information).

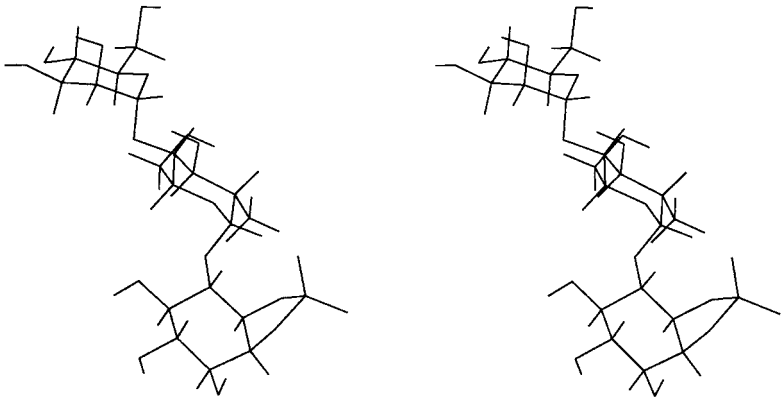

Figure 11. Stereoview of the AMBER global minimum of compound **4**.

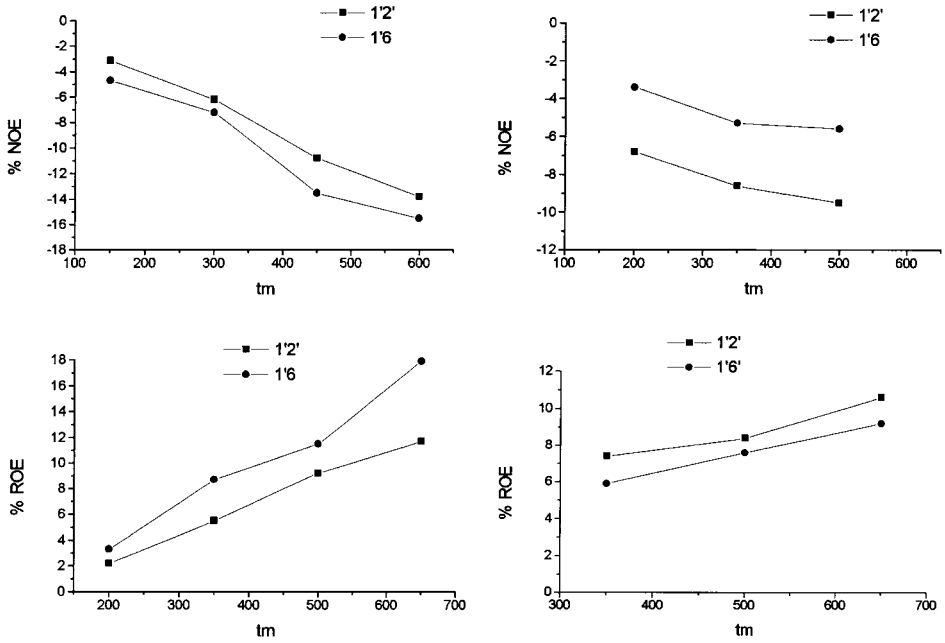

Figure 12. Build up curves of the behavior of the key intra- and interresidue NOE and ROEs of compound **1** in [D_6]DMSO (left) and in [D_{18}]SDS micelles.

The observed NOEs (Table 7) were basically identical to those mentioned above for the corresponding oligosaccharides and, therefore, are in agreement with conformational behavior within the limits described for the free trisaccharide **4**.

Table 7. Experimental 1D-NOESY and 1D-T-ROESY intensities [%] for compound **2** in DMSO at 30° C.

	NOESY		T-ROESY	
Proton Pairs	400 ms	600 ms	300 ms	500 ms
H1′/H6	7.6	19.5	9.2	13.1
H1″/H4′	not determined	15.6	8.3	13.7

Experimental Section

General methods: Melting points were determined on a Kofler hot-stage apparatus and are uncorrected. Optical rotations were determined with a Perkin-Elmer 141 polarimeter. Elemental analyses were obtained with a Perkin-Elmer 240 instrument. FAB mass spectral data were obtained on a VG Autoespec high-resolution mass spectrometer. Separation and purification of products was performed by flash chromatography using silica gel (Merck, 230–400 mesh) or Florisil adsorbent (Fluka, 100–200 mesh). Silica gel plates (Merck, GF_{254}) were used for analytical thin-layer chromatography (TLC). Tetrahydrofuran (THF) and ethyl ether (Et_2O) were distilled under argon from sodium-benzophenone, methanol (MeOH) from magnesium, dimethylformamide (DMF), and pyridine from barium oxide, and dimethyl sulfoxide (DMSO) was dried over 4 Å molecular sieves. All reactions were performed under an argon atmosphere by using anhydrous, freshly distilled solvents, unless otherwise indicated.

Phenyl 2-azido-3,4,6-tri-*O*-benzyl-2-deoxy-1-thio-*α*/*β*-D-glucopyranoside (10):[22] To a solution of compound **9**[22] (70 mg, 162 μmol) in benzene (3 mL) were added 20% aqueous NaOH (1.5 mL) and $n$$Bu_4NHSO_4$ (30 mg, 94 μmol) with vigorous stirring. After 1 h, BnBr (78 μL, 660 μmol) was added within 10 min by syringe, and the mixture was left to stir for 14 h. Then, the reaction mixture was diluted with water (10 mL) and toluene (25 mL). The organic layer was separated, successively washed with water (5 mL), aqueous 1M HCl (2 × 5 mL), and water (2 × 5 mL), dried over Na_2SO_4, and evaporated. The crystalline residue was taken up in the eluent with the aid of some drops of DMF, and purified by flash chromatography (hexane/EtOAc 8:1) to give **10**[22] (85 mg, 93%) as a colorless powder.

2-Azido-3,4,6-tri-*O*-benzyl-2-deoxy-*α*/*β*-D-glucopyranose (11):[21] To a solution of **10** (53 mg, 93 μmol) in acetone/water (5 mL; 99:1) was added NBS (27 mg, 151 μmol) at −15°C. The reaction mixture was stirred under exclusion of light until an orange color appeared (approx. 20 min), then quenched with aqueous saturated $NaHCO_3$ (10 mL), and extracted with EtOAc (2 × 30 mL). The organic layers were combined, washed with brine (15 mL), dried over Na_2SO_4, and evaporated. The residue was purified by flash chromatography (hexane/EtOAc 5:2) to give **11**[21] (37 mg, 84%) as a colorless solid: TLC (hexane/EtOAc 3:1): $R_f = 0.26$.

***O*-(2-Azido-3,4,6-tri-*O*-benzyl-2-deoxy-*α*/*β*-D-glucopyranosyl) trichloroacetimidate (12)**:[21] Compound **11** (37 mg, 78 μmol) in CH_2Cl_2 (4 mL) was treated with CCl_3CN (81 μL, 812 μmol) and K_2CO_3 (70 mg, 506 μmol) as described for **8**. After 4 h, the reaction mixture was processed and the residue thus obtained was chromatographed on Florisil (hexane/EtOAc 4:1) to give **12**[21] (43 mg, 92%) as a colorless oil.

Phenyl *O*-(2,3,4,6-tetra-*O*-benzyl-*α*-D-mannopyranosyl)-(1→4)-2-azido-3,6-di-*O*-benzyl-2-deoxy-1-thio-*α*-D-glucopyranoside (15): A mixture of **13**[24] (372 mg, 778 μmol), **14**[22] (640 mg, 934 μmol), and freshly activated, powdered 4 Å molecular sieves (300 mg) was added to Et_2O (10 mL) and stirred for 1 h at room temperature. Then the stirred mixture was treated with TMSOTf (375 μL of a 0.2M solution in Et_2O, 75 μmol). After 1 h, $NaHCO_3$ (500 mg) was added, and stirring was continued for 10 min. The reaction mixture was filtered through a pad of Celite, and the filter bed was washed with CH_2Cl_2 (2 × 25 mL). The filtrate and the washings were combined, washed with brine (30 mL), dried (Na_2SO_4), and concentrated to dryness. The residue was purified by flash chromatography (toluene/EtOAc 30:1) to give **15** (482 mg, 62%) as a colorless syrup: TLC (toluene/EtOAc 8:1): $R_f = 0.60$; $[\alpha]_D^{22} = +88.0$ ($c = 1.0$, $CHCl_3$); ^{1}H NMR (300 MHz, $CDCl_3$): $\delta = 7.57-7.54$ (m, 2H), 7.36–7.19 (m, 33H), 5.59 (d, 1H, $J =$ 5.4 Hz), 5.31 (d, 1H, $J = 2.3$ Hz), 4.96 (d, 1H, $J = 11.2$ Hz), 4.85 (d, 1H, $J = 10.9$ Hz), 4.68–4.28 (m, 11H), 4.38 (ddd, 1H, $J = 9.9$, 4.8, 2.0 Hz), 4.30 (d, 1H, $J = 12.1$ Hz), 4.02–3.62 (m, 11H). MS-FAB (thioglycerol matrix, NaI): m/z : 1022 ([MNa]$^+$).

***O*-(2,3,4,6-Tetra-*O*-benzyl-*α*-D-mannopyranosyl)-(1→4)-2-azido-3,6-di-*O*-benzyl-2-deoxy-*α*/*β*-D-glucopyranose (16)**: To a solution of **15** (375 mg, 375 μmol) in acetone/water (25 mL; 99:1) was added NBS (130 mg, 728 μmol) at −15°C. The reaction mixture was stirred under exclusion of light for 90 min and then worked up as described for **11**. The crude product was purified by flash chromatography (hexane/EtOAc 5:2–2:1) to give **16** (300 mg, 88%; $\alpha/\beta = 1.5:1$ by ^{1}H NMR spectroscopy) as a colorless syrup: TLC (toluene/EtOAc 8:1): $R_f = 0.11$; TLC (hexane/EtOAc 3:1): $R_f = 0.20$; $[\alpha]_D^{20} = +18.8$ ($c = 1.0$, $CHCl_3$); ^{1}H NMR (300MHz, $CDCl_3$): $\delta =$ 7.35–7.17 (m, 30H), 5.32–4.22(m, 14H), 5.32(t, 1H, J = 3.4Hz), 5.29 (d, 1H, $J = 2.4$ Hz), 5.27 (d, 1H, $J = 2.4$ Hz), 4.94 (d, 1H, $J = 11.3$ Hz), 4.92 (d, 1H, $J = 11.3$ Hz), 4.84 (d, 1H, $J = 10.9$ Hz), 4.82 (d, 1H, $J = 11.0$ Hz), 3.98–3.31 (m, 13H), 4.05 (ddd, 1H, J = 9.6, 5.3, 2.1 Hz), 3.44 (bd, 1H, J = 3.5 Hz); ^{13}C NMR (50 MHz, $CDCl_3$): $\delta = 138.49$, 138.42, 138.35, 138.02, 137.87, 137.82, 137.76, 128.46–127.00 (phenyl), 100.52, 100.40, 96.171, 91.917, 82.85, 79.85, 79.55, 79.46, 77.77, 74.87, 74.66, 74.47, 73.40, 73.32, 73.12, 72.37, 72.20, 70.24, 69.60, 69.46, 69.31, 67.26, 63.88; MS-FAB (thioglycerol matrix, NaI): m/z: 931 ([MNa]$^+$).

***O*-(2,3,4,6-Tetra-*O*-benzyl-*α*-D-mannopyranosyl)-(1→4)-2-azido-3,6-di-O-benzyl-2-deoxy-D-glucopyranosyl trichloroacetimidate (17)**: Compound **16** (270 mg, 297 μmol) in CH_2Cl_2 (15 mL) was treated with CCl_3CN (1 mL,

0947-6539/99/0501-0330 $ 17.50+.50/0 *Chem. Eur. J.* **1999**, *5*, No. 1

6.93 mmol) and K_2CO_3 (74 mg, 535 μmol) as described for **8**. After 4 h, the reaction mixture was processed, and the obtained residue was rapidly chromatographed (hexane/EtOAc 4:1 + 1% Et_3N) to give **17** (263 mg, 84%; $\alpha/\beta = 1:5$ by ^1H NMR spectroscopy) as a colorless syrup: TLC (hexane/EtOAc 3:1): $R_f = 0.75$; $[\alpha]_D^{20} = +16.2$ ($c = 1.0$, $CHCl_3$); ^1H NMR (300 MHz, $CDCl_3$): $\delta = 8.75$ (s, 1H), 8.74 (s, 1H), 7.23–7.16 (m, 30H), 6.43 (d, 1H, $J = 3.4$ Hz), 5.66 (d, 1H, $J = 8.3$ Hz), 5.32 (d, 1H, $J = 2.2$ Hz), 4.94–4.26 (m, 12H), 4.92 (d, 1H, $J = 11.5$ Hz), 4.82 (d, 1H, $J = 10.7$ Hz), 4.01–3.39 (m, 12H), 3.42 (dd, 1H, $J = 9.6$, 8.9 Hz).

1,2-*O*-(L-1,7,7-Trimethyl[2.2.1]bicyclohept-6-ylidene)-D-*myo*-inositol (18): Compound **18** was prepared following a known procedure,[26,27] with modified work up in order to obtain pure product as follows. To a suspension of dry *myo*-inositol (3.68 g, 20.4 mmol) in DMSO (40 mL) L-camphor dimethyl ketal[58] (8.09 g, 40.8 mmol) and concentrated H_2SO_4 (33 μL) were added, and the resulting heterogenous mixture was stirred at 55–60 °C for 3 h. After adding Et_3N (660 μL), the reaction mixture was concentrated in vacuo. Then $CHCl_3$/MeOH/H_2O (50:5:1, 67 mL) was added to the residue, and the mixture was homogenized by sonication. *p*-Toluenesulfonic acid (13.3 mg, 69.7 μmol) was then added and the solution was stirred at room temperature overnight to give a white precipitate. After quenching the reaction with Et_3N (330 μL), the solution was filtered with suction, the precipitate was washed with $CHCl_3$ (2 × 50 mL), and dried in vacuo. In order to remove *myo*-inositol from the crude product, the precipitate (4.58 g) was mixed with Florisil adsorbent (50 mL), wetted with $CHCl_3$/MeOH/Et_3N 40:4:1, homogenized by sonication and chromatographed ($CHCl_3$/MeOH/Et_3N 40:10:1 → 30:10:1). Evaporation of the filtrate and crystallization of the residue from MeOH/Et_3N 50:1 yielded three crops of pure **18**[26,27] (1.86 g, 29% in total) as clear crystals: m.p. 256–257 °C; TLC ($CHCl_3$/MeOH 4:1): $R_f = 0.36$; $[\alpha]_D^{23} = -40.3$ ($c = 1.0$, pyridine); NMR data were in accordance with with those described for the enantiomer;[27] elemental analysis calcd for $C_{16}H_{26}O_6$: C 61.12, H 8.34; found C 61.12, H 8.35.

3,4-*O*-(1,1,3,3-Tetraisopropyldisiloxanedi-1,3-yl)-1,2-*O*-(L-1,7,7-trimethyl-[2.2.1]bicyclohept-6-ylidene)-D-*myo*-inositol (19): Compound **19** was prepared as described for its enantiomer.[27] A solution of **18** (716 mg, 2.28 mmol) in dry pyridine (7 mL) was treated with $TIPDSCl_2$ (865 μL, 2.76 mmol) at −30 °C. The mixture was allowed to warm to room temperature over 30 min and stirring was continued at room temperature for 3.5 h. The reaction mixture was diluted with EtOAc (25 mL) and washed with water (3 × 10 mL). The organic extracts were combined, dried (Na_2SO_4), and evaporated. The residue was purified by flash chromatography to give **19** (1.18 g, 93%) as a colorless, crystalline foam: TLC (hexane/EtOAc 2:1): $R_f = 0.45$; $[\alpha]_D^{22} = -8.6$ ($c = 0.5$, $CHCl_3$); NMR data were in accordance with those described for the enantiomer;[27] elemental analysis calcd for $C_{28}H_{52}O_7Si_2$: C 60.39, H 9.41; found C 60.10, H 9.30.

***O*-(3,4,6-Tri-*O*-acetyl-2-azido-2-deoxy-α-D-glucopyranosyl)-(1→6)-3,4-*O*-(1,1,3,3-tetraisopropyldisiloxanedi-1,3-yl)-1,2-*O*-(L-1,1,7-trimethyl[2.2.1]-bicylohept-6-ylidene)-D-*myo*-inositol (20a) and *O*-(3,4,6-tri-*O*-acetyl-2-azido-2-deoxy-α-D-glucopyranosyl)-(1→5)-3,4-*O*-(1,1,3,3-tetraisopropyldisiloxanedi-1,3-yl)-1,2-*O*-(L-1,7,7-trimethyl [2.2.1]bicyclohept-6-ylidene)-D-*myo*-inositol (20b)**: A mixture of **19** (1.055 g, 1.89 mmol), **8** (740 mg, 1.55 mmol), and freshly activated, powdered 3 Å molecular sieves (750 mg) was added to Et_2O (25 mL) and stirred for 45 min at room temperature. The mixture was then cooled to −20 °C and treated with TMSOTf (775 μL of a 0.2 M solution in Et_2O, 155 μmol). After the mixture had been stirred at −20 °C for 30 min, $NaHCO_3$ (500 mg) was added, and the solution was allowed to cool to room temperature. The reaction mixture was filtered through a pad of Celite, and the filter bed was washed with CH_2Cl_2 (2 × 25 mL). The filtrate and the washings were combined, washed with brine (30 mL), dried (Na_2SO_4), and concentrated to dryness. The residue was purified by flash chromatography (hexane/EtOAc 5:1 9%) as a colorless, slowly crystalizing syrup.

20a: TLC (hexane/EtOAc 2:1): $R_f = 0.66$; $[\alpha]_D^{23}$ +80.6 ($c = 1.0$, $CHCl_3$); ^1H NMR (200 MHz, $CDCl_3$): $\delta = 5.55$ (d, 1H, $J = 3.5$ Hz), 5.53 (dd, 1H, $J = 10.6$, 9.2 Hz), 5.04 (dd, 1H, $J = 10$, 9.2 Hz), 4.67 (ddd, 1H, $J = 10$, 4.7, 2.0 Hz), 4.27 (dd, 1H, $J = 12.4$, 4.7 Hz), 4.20 (dd, 1H, $J = 5.2$, 3.8 Hz), 4.15–4.02 (m, 2H), 3.94 (dd, 1H, $J = 9.2$, 3.8 Hz), 3.84 (t, 1H, $J = 9$ Hz), 3.77 (dd, 1H, $J = 10.3$, 6.5 Hz), 3.42 (dt, 1H, $J = 9.4$, 1.4 Hz), 3.30 (dd, 1H, $J = 10.6$, 3.5 Hz), 2.57 (d, 1H, 1.4 Hz), 2.10, 2.07, and 2.03 (3s, 3H each), 2.10–0.89 (m, 38H), 0.86 (s, 6H); ^{13}C NMR (50 MHz, $CDCl_3$): $\delta = 170.70$, 169.98, 169.75, 117.75, 96.07, 79.97, 76.99, 76.18, 75.80, 72.67, 72.02, 70.46, 68.69, 67.20, 62.17, 61.03, 51.51, 47.99, 45.24, 45.13, 29.56, 27.01, 20.67, 20.58, 20.44, 20.12, 17.50, 17.32, 17.25, 17.16, 17.06, 16.98, 12.90, 12.72, 12.20, 11.99, 9.68; elemental analysis calcd for $C_{40}H_{67}N_3O_{14}Si_2$: C 55.21, H 7.76, N 4.83; found C 55.20, H 7.70, N 4.58.

20b: TLC (hexane/EtOAc 2:1): $R_f = 0.46$; TLC (toluene/acetone 9:1): $R_f = 0.33$; $[\alpha]_D^{22} = +59.2$ ($c = 1.0$, $CHCl_3$); ^1H NMR (200 MHz, $CDCl_3$): $\delta = 5.61$ (d, 1H, $J = 3.7$ Hz), 5.50 (dd, 1H, $J = 10.5$, 9.1 Hz), 5.01 (dd, 1H, $J = 10.4$, 9.1 Hz), 4.79 (dt, 1H, $J = 10.5$, 3.2 Hz), 4.25–4.01 (m, 4H), 3.90 (dd, 1H, $J = 9.4$, 4.0 Hz), 3.79 (t, 1H, $J = 6.1$ Hz), 3.70–3.60 (m, 1H), 3.54–3.45 (m, 2H), 3.37 (dd, 1H, $J = 10.5$, 3.9 Hz), 2.09, 2.08, and 2.01 (3s, 3H each), 2.10–0.98 (m, 38H), 0.86, 0.81 (2s, 3H each); ^{13}C NMR (50 MHz, $CDCl_3$): $\delta = 170.74$, 169.91, 169.75, 118.13, 97.55, 77.51, 77.20, 76.80, 76.47, 76.07, 75.20, 73.16, 70.78, 68.62, 67.14, 61.92, 61.07, 51.58, 48.08, 45.11, 29.66, 29.45, 26.96, 20.83, 20.67, 20.62, 20.41, 19.99, 17.67, 17.55, 17.31, 17.20, 17.11, 13.00, 12.71, 12.43, 11.97, 9.79; elemental analysis calcd for $C_{40}H_{67}N_3O_{14}Si_2$: C 55.21, H 7.76, N 4.83; found C 55.40, H 7.56, N 4.58.

***O*-(2-Azido-3,4,6-tri-*O*-benzyl-2-deoxy-α-D-glucopyranosyl)-(1→6)-3,4-*O*-(1,1,3,3-tetraisopropyldisiloxanedi-1,3-yl)-1,2-*O*-(L-1,7,7-trimethyl-[2.2.1]bicyclohept-6-ylidine)-D-*myo*-inositol (21a), *O*-(2-azido-3,4,6-tri-*O*-benzyl-2-deoxy-α-D-glucopyranosyl)-(1→5)-3,4-*O*-(1,1,3,3-tetraisopropyl-disiloxanedi-1,3-yl)-1,2-*O*-(L-1,7,7-trimethyl[2.2.1]bicyclohept-6-ylidene)-D-*myo*-inositol (21b), and *O*-(2-azido-3,4,6-tri-*O*-benzyl-2-deoxy-β-D-glucopyranosyl)-(1→6)-3,4-*O*-(1,1,3,3-tetraisopropyldisiloxanedi-1,3-yl)-1,2-*O*-(L-1,7,7-trimethyl[2.2.1]bicyclohept-6-ylidene)-D-*myo*-inositol (21c)**: A mixture of **19** (1.39 g, 2.50 mmol), **12** (1.25 g, 2.08 mmol), and freshly activated, powdered 3 Å molecular sieves (750 mg) was added to Et_2O (30 mL) and stirred for 1 h at room temperature. The mixture was cooled to −40 °C and treated with TMSOTf (416 μL of a 0.1% M solution in Et_2O, 41.6 μmol). After stirring for 30‰min, the reaction mixture was quenched with $NaHCO_3$ (1 g), and warmed to room temperature. The mixture was filtered through a pad of Celite, the filter bed was washed with CH_2Cl_2 (2 × 50 mL) and the combined filtrates were evaporated. The residue was chromatographed (hexane/EtOAc 10:1–9:1–6:1) To give **21a** (1.42 g, 67% as a colorless, glassy foam, **21b** (147 mg, 7%) as a colorless syrup, and **21c** (359 mg, 17%) as a colorless foam).

21a: TLC (hexane/EtOAc 3:1): $R_f = 0.75$; $[\alpha]_D^{23} = +49.1$ ($c = 0.35$, $CHCl_3$); ^1H NMR (200 MHz, $CDCl_3$): $\delta = 7.40–7.17$ (m, 15H), 5.48 (d, 1H, $J = 3.6$ Hz), 4.88–4.47 (m, 6H), 4.39–4.30 (m, 1H), 4.23 (dd, 1H, $J = 5.4$, 3.5 Hz), 4.10–3.72 (m, 7H), 3.64 (dd, 1H, $J = 10.8$, 1.9 Hz), 3.43 (dt, 1H, $J = 9.1$, 1.8 Hz), 3.41 (dd, 1H, $J = 10.1$, 3.6 Hz), 2.55 (d, 1H, $J = 1.8$ Hz), 2.05–0.90 (m, 38H), 0.88, 0.87 (2s, 3H each); ^{13}C NMR (50 MHz, $CDCl_3$): $\delta = 138.35$, 138.17, 128.42–127.58 (phenyl), 117.78, 96.27, 80.32, 79.69, 78.1, 77.00, 76.25, 75.79, 75.36, 74.84, 73.38, 72.83, 72.51, 70.41, 68.32, 63.64, 51.55, 48.01, 45.18, 29.59, 27.08, 20.49, 20.18, 17.54, 17.36, 17.29, 17.21, 17.11, 17.03, 12.96, 12.73, 12.29, 12.06, 9.73; elemental analysis calcd for $C_{55}H_{79}N_3O_{11}Si_2$: C 65.12, H 7.85, N 4.14; found: C 64.80, H 7.72, N 4.10.

21b: TLC (hexane/EtOAc 3:1): $R_f = 0.53$; ^1H NMR (200 MHz, $CDCl_3$): $\delta = 7.37–7.14$ (m, 15H), 5.40 (d, 1H, $J = 3.9$ Hz), 4.86–4.46 (m, 6H), 4.30–3.40 (m, 12H), 3.97 (dd, 1H, $J = 10.2$, 8.9 Hz), 3.02–2.98 (m, 1H), 2.10–1.00 (m, 38H), 0.86, 0.83 (2s, 3H each).

21c: TLC (hexane/EtOAc 3:1): $R_f = 0.67$; $[\alpha]_D^{22} = -13.0$ ($c = 1.0$, $CHCl_3$); ^1H NMR (200 MHz, $CDCl_3$): $\delta = 7.37–7.13$ (m, 15H), 4.92–4.43 (m, 7H), 4.78 (d, 1H, $J = 7.8$ Hz), 4.23 (dd, 1H, $J = 5.4$, 3.7 Hz), 4.03–3.87 (m, 3H), 3.82–3.67 (m, 4H), 3.57–3.38 (m, 4H), 2.78 (s, 1H), 2.35–1.00 (m, 38H), 0.85 (s, 6H); ^{13}C NMR (50 MHz, $CDCl_3$): $\delta = 138.18$, 128.36–127.57 (phenyl), 117.40, 102.12, 83.35, 82.80, 77.78, 77.40, 77.20, 76.77, 75.50, 74.40, 73.57, 72.95, 68.95, 66.33, 66.30, 51.55, 48.03, 45.23, 45.14, 29.64, 29.11, 27.06, 20.50, 20.19, 17.54, 17.42, 17.37, 17.21, 17.11, 17.02, 12.97, 12.73, 12.31, 12.04, 9.92; elemental analysis calcd for $C_{55}H_{79}N_3O_{11}Si_2$: C 65.12, H 7.85, N 4.14; found: C 64.98, H 7.85, N 4.40.

***O*-(2,3,4,6-Tetra-*O*-benzyl-α-D-mannopyranosyl)-(1→4)-*O*-(2-azido-3,6-tri-*O*-benzyl-2-deoxy-β-D-glucopyranosyl)-(1→6)-3,4-*O*-(1,1,3,3-tetraiso-propyldisiloxanedi-1,3-yl)-1,2-*O*-(L-1,7,7-trimethyl[2.2.1]bicyclohept-6-yli-dine)-D-*myo*-inositol (22a) and *O*-(2,3,4,6-tetra-*O*-benzyl-α-D-manno-pyranosyl)-(1→4)-*O*-(2-azido-3,6-tri-*O*-benzyl-2-deoxy-β-D-glucopyrano-syl)-(1→6)-3,4-*O*-(1,1,3,3-tetraisopropyldisiloxanedi-1,3-yl)-1,2-*O*-(L-1,7,7-trimethyl[2.2.1]bicyclohept-6-ylidine)-D-*myo*-inositol (22b)**: A mixture of **19** (180 mg, 321 μmol), 17 (263 mg, 250 μmol), and freshly activated, powdered 4 Å molecular sieves (180 mg) was added to Et_2O (4 mL), and stirred for 30 min at room temperature. Then, the mixture was cooled to −

40 °C and treated dropwise with TMSOTf (416 μL of a 0.1‰M solution in Et_2O, 41.6 μmol). After stirring for 30 min, the reaction mixture was processed as described for **15**. The obtained residue was chromatographed (toluene/EtOAc 25:1, 2.5 × 21 cm) to give **22a** (235 mg, 65 %) as a colorless syrup, and **22b** (105 mg, 29 %) as a colorless syrup.

22a: TLC (toluene/EtOAc 10:1): $R_f = 0.54$; $[\alpha]_D^{20} = +39.3$ ($c = 1.0$, $CHCl_3$); ^{1}H NMR (300 MHz, $CDCl_3$): $\delta = 7.34-7.15$ (m, 30H), 5.49 (d, 1H, $J =$ 3.6 Hz), 5.31 (d, 1H, $J = 2.1$ Hz), 4.93 (d, 1H, $J = 11.2$ Hz), 4.82 (d, 1H, $J =$ 10.8 Hz), 4.65–4.25 (m, 11H), 4.21 (bt, 1H, $J = 4.2$ Hz), 4.07–3.67 (m, 13H), 3.60 (dt, 1H, $J = 10.8$, 1.9 Hz), 3.42 (dt, 1H, $J = 9.6$, 1.5 Hz), 3.34 (dd, 1H, $J = 9.9$, 3.4 Hz), 2.57 (d, 1H, $J = 1.8$ Hz), 1.94–0.98 (m, 38H), 0.85, 0.83 (2 s, 3H each); ^{13}C NMR (50 MHz, $CDCl_3$): $\delta = 138.58$, 138.52, 138.44, 137.99, 128.41–126.89 (phenyl), 117.78, 100.32, 95.86, 80.04, 79.82, 79.43, 77.42, 76.26, 76.10, 75.73, 75.04, 74.84, 74.04, 73.29, 73.05, 72.86, 72.21, 72.04, 69.92, 69.18, 68.81, 63.33, 51.52, 47.97, 45.25, 45.12, 29.52, 27.04, 20.15, 17.52, 17.39, 17.26, 17.20, 17.08, 17.00, 12.94, 12.68, 12.24, 12.01, 9.64; elemental analysis calcd for $C_{82}H_{107}N_3O_{16}Si_2$: C 68.07, H 7.45, N 2.90; found: C 68.37, H 7.71, N 2.89.

22b: TLC (toluene/EtOAc 10:1): $R_f = 0.61$; $[\alpha]_D^{20} = -5.3$ ($c = 1.0$, $CHCl_3$); ^{1}H NMR (300 MHz, $CDCl_3$): $\delta = 7.32-7.14$ (m, 30H), 5.28 (d, 1H, $J =$ 2.0 Hz), 4.95 (d, 1H, $J = 11.4$ Hz), 4.82 (d, 1H, $J = 10$ Hz), 4.82 (d, 1H, $J =$ 8.3 Hz), 4.61–3.39 (m, 27H), 4.21 (dd, 1H, $J = 5.1$, 4.2 Hz), 3.28 (dd, 1H, $J = 9.8$, 8.8 Hz), 2.74 (d, 1H, $J = 1.5$ Hz), 2.08–0.95 (m, 38H), 0.81, 0.80 (2 s, 3 H each); ^{13}C NMR (50 MHz, $CDCl_3$): $\delta = 138.61$, 138.56, 138.51, 138.44, 138.12, 128.42–126.93 (phenyl), 117.47, 101.88, 100.22, 83.12, 82.41, 79.69, 77.44, 76.79, 76.61, 76.13, 75.53, 74.96, 74.92, 74.85, 74.44, 73.40, 73.34, 72.97, 72.91, 72.29, 72.09, 69.83, 69.51, 66.04, 51.52, 48.03, 45.21, 45.10, 29.54, 27.06, 20.51, 20.18, 17.53, 17.43, 17.38, 17.31, 17.20, 17.10, 17.02, 12.96, 12.72, 12.30, 12.04, 9.83; elemental analysis calcd for $C_{82}H_{107}N_3O_{16}Si_2$: C 68.07, H 7.45, N 2.90; found: C 68.15, H 7.64, N 2.80.

***O*-(3,4,6-Tri-*O*-acetyl-2-azido-2-deoxy-α-D-glucopyranosyl)-(1→6)-3,4-5-tri-*O*-acetyl-1,2-*O*-(L-1,7,7-trimethyl[2.2.1]bicyclohept-6-ylidine)-D-*myo*-inositol** (**23**): A solution of **20a** (220 mg, 253 mmol) in THF (8 mL) was treated at 0 °C with Bu_4NF (556 μL of a 1‰M solution in THF, 556 μmol). After 30 min, pyridine (8 mL) and acetic anhydride (5 mL) were added, and the mixture was allowed to come to room temperature. After stirring for 20 h at room temperature, the reaction mixture was co-evaporated with toluene (3 × 40 mL), and the residue was purified by flash chromatography (hexane/EtOAc 3:2, 2.0 × 9.5 cm) to give **23** (190 mg, quantitative) as a colorless foam: TLC (hexane/EtOAc 3:2): $R_f = 0.31$; $[\alpha]_D^{18} = +102.5$ (c = 1.0, $CHCl_3$); ^{1}H NMR (300 MHz, $CDCl_3$): $\delta = 5.52$ (d, 1H, $J = 3.5$ Hz, Hb-1), 5.32 (t, 1H, $J = 9.2$ Hz, Ha-4), 5.29 (dd, 1H, $J = 10.6$, 9.2 Hz, Hb-3), 5.15 (dd, 1H, $J = 9.2$, 4.2 Hz, Ha-3), 5.07 (dd, 1H, $J = 9.8$, 8.5 Hz, Ha-5), 4.98 (dd, 1H, $J = 10.3$, 9.2 Hz, Hb-4), 4.48 (dd, 1H, $J = 6.2$, 4.3 Hz, Ha-2), 4.19–4.11 (m, 3H, Ha-1, Hb-6,-6′), 4.06 (dt, 1H, $J = 10.3$, 3.3 Hz, Hb-5), 3.99 (dd, 1H, $J = 9.8$, 6.8 Hz, Ha-6), 3.38 (dd, 1H, $J = 10.6$, 3.5 Hz, Hb-2), 2.08, 2.07, 2.05, 2.04, 2.02, 2.00 (6 s, 3 H each), 1.92–1.63 (m, 4H), 1.46–1.35 (m, 2H), 1.24–1.14 (m, 2H), 0.94, 0.90, 0.85 (3s, 3 H each); ^{13}C NMR (50 MHz, $CDCl_3$): $\delta = 170.60$, 169.77, 169.61, 169.51, 169.24, 118.80, 95.52, 76.12, 75.07, 72.70, 70.82, 70.20, 69.81, 69.04, 68.40, 68.14, 61.81, 60.92, 51.52, 47.96, 45.00, 44.51, 29.71, 26.87, 20.65, 20.56, 20.41, 20.27, 20.20, 9.52; elemental analysis calcd for $C_{34}H_{47}N_3O_{16}$: C 54.18, H 6.29, N 5.57; found: C 54.42, H 6.56, N 5.47.

***O*-(2-Azido-3,4,6-tri-*O*-benzyl-2-deoxy-α-D-glucopyranosyl)-(1→6)-3,4-5-tri-*O*-benzyl-1,2-*O*-(L-1,7,7-trimethyl[2.2.1]bicyclohept-6-ylidine)-D-*myo*-inositol** (**24**): Method a: To a stirred solution of **23** (230 mg, 305 μmol) in methanol (50 mL) was added sodium methoxide (10 drops of a 0.5‰M solution in methanol) After 5 h, the solution was neutralized as with gaseous carbon dioxide, treated with 2 drops of Et_3N, concentrated and coevaporated with toluene (2 × 10 mL). The residue was taken up in DMF (5 mL) and treated with BnBr (325 μL, 2.75 mmol) and portions of 95 % NaH (93 mg, 3.66 mmol). After 4 h, more BnBr (250 μL, 2.12 mmol) was added, and the reaction mixture was left stirring for another 3 h. The reaction was quenched by slow addition of 10 drops MeOH, then H_2O (10 drops) and NH_4Cl (200 mg). The reaction mixture was filtered through a pad of Celite and the filter cake was washed with EtOAc (2 × 20 mL). The combined filtrates were evaporated at reduced pressure and the residue was purified by flash chromatography (hexane/EtOAc 10:1–6:1) to give **24** (285 mg, 90 %) as a colorless syrup: TLC (hexane/EtOAc 4:1): $R_f = 0.47$; $[\alpha]_D^{19} = +53.3$ ($c = 1.0$, $CHCl_3$); ^{1}H NMR (200 MHz, $CDCl_3$): $\delta = 7.45-7.08$ (m, 30H), 5.67 (D, 1H, $J = 3.6$ Hz), 4.93–4.56 (m, 11H), 4.44 (d,1H, $J =$ 12.2 Hz), 4.40–4.33 (m, 1H),4.20–4.00 (m, 4H), 3.94–3.80 (m, 3H), 3.45 (dd, 1H, $J = 10.2$, 3.6 Hz), 3.65–3.41 (m, 4H), 2.10–0.90 (m, 16H), 1.15, 0.95, 0.94 (3s, 3H each); ^{13}C NMR (50 MHz, $CDCl_3$): $\delta = 138.48$, 138.35, 138.03, 137.99, 128.36–127.45 (phenyl), 118.04, 95.68, 80.82, 80.58, 79.94, 78.29, 78.07, 76.96, 76.12, 75.18, 74.76, 74.59, 73.84, 73.37, 72.51, 70.40, 67.95, 63.38, 51.58, 47.93, 45.15, 44.75, 29.87, 26.96, 20.58, 20.37, 9.73.

Method b: A solution of **21a** (75 mg, 73.9 mmol) in THF (2 mL) was treated at 0 °C with Bu_4NF (155 μL of a 1‰M solution in THF, 155 μmol). After 30 min, DMF (2 mL) was added, and THF was removed by evaporation. 95 % NaH (11.2 mg, 443 μmol) and BnBr (53 μL, 443 μmol) were added, and the mixture was stirred at room temperature. After 16 h, more 95 % NaH (10 mg, 396 μmol) and BnBr (30 μL, 252 μmol) were added, and the reaction mixture was left stirring for another 4 h. After quenching with MeOH (100 μL) and NH_4Cl (100 mg), the mixture was evaporated in high vacuum, and the residue was purified by flash chromatography (hexane/EtOAc 10:1) to give **23** (55 mg, 72 %), identical with the product described above.

***O*-(2-Azido-3,4,6-tri-*O*-benzyl-2-deoxy-β-D-glucopyranosyl)-(1→6)-3,4-5-tri-*O*-benzyl-1,2-*O*-(L-1,7,7-trimethyl[2.2.1]bicyclohept-6-ylidine)-D-*myo*-inositol** (**25**): A solution of **21c** (62 mg,61.1 mmol) in THF (2 mL) was treated at 0 °C with Bu_4NF(134 μL of a 1M solution in THF, 134 μmol). After 45 min, pyridine (4 mL) and acetic anhydride (2 mL) were added, and the mixture was allowed to come to room temperature. After stirring for 22 h, the reaction mixture was co-evaporated with toluene (3 × 20 mL) and the residue was purified by flash chromatography (hexane/EtOAc 4:1) to give **25** (47 mg, 86 %) as a colorless syrup: TLC (hexane/EtOAc 3:1): $R_f = 0.40$; $[\alpha]_D^{22} = +10.8$ ($c = 1.0$, $CHCl_3$); ^{1}H NMR (200 MHz, $CDCl_3$): $\delta =$ 7.30–7.06 (m, 15H), 5.37 (dd, 1H, $J = 10.2$, 8.0 Hz, Ha-4), 5.09 (dd, 1H, $J =$ 10.2, 4.1 Hz, Ha-3), 5.02 (t, 1H, $J = 8$ Hz, Ha-5), 4.82–4.69 (m, 3H), 4.55–4.37 (m, 3H), 4.15 (t, 1H, $J = 6$ Hz), 3.91 (dd, 1H, $J = 7.2$, 5.6 Hz), 3.66–3.57 (m, 3H), 3.36–3.30 (m, 3H), 2.02–0.80 (m, 25H), 1.98, 1.96 (2 s, 9H), 0.89, 0.87, 0.78 (3 s, 3 H each); ^{13}C NMR (50 MHz, $CDCl_3$): $\delta = 169.94$, 169.83, 169.74, 137.93, 128.38–127.65 (phenyl), 118.09, 101.65, 83.22, 78.85, 77.50, 75.44, 75.11, 74.93, 73.92, 73.45, 73.29, 72.29, 69.48, 69.24, 68.38, 66.55, 51.52, 47.95, 45.10, 43.94, 29.79, 26.92, 20.82, 20.67, 20.62, 20.25, 20.21, 17.03, 9.88; Elemental analysis calcd for $C_{49}H_{59}N_3O_{13}$: C 65.48, H 6.62, N 4.68; found: C 65.13, H 6.94, N 4.65.

***O*-(2,3,4,6-Tetra-*O*-benzyl-α-D-mannopyranosyl)-(1→4)-*O*-(2-azido-3,6-tri-*O*-benzyl-2-deoxy-β-D-glucopyranosyl)-(1→6)-3,4-5-tri-*O*-benzyl-1,2-*O*-(L-1,7,7-trimethyl[2.2.1]bicyclohept-6-ylidine)-D-*myo*-inositol** (**26**): A solution of **22a** (215 mg, 148 μmol) in THF (8 mL) was treated at 0 °C with Bu_4NF(327 μL of a 1M solution in THF, 327 μmol). After 45 min, pyridine (8 mL) and acetic anhydride (5 mL) were added, and the mixture was allowed to come to room temperature. After stirring for 20 h, the reaction mixture was coevaporated with toluene (3 × 40 mL) and the residue was purified by flash chromatography (hexane/EtOAc 4:1, 2.0 × 15.0 cm) to give **26** (186 mg, 95 %) as a colorless syrup: TLC (toluene/EtOAc 10:1): $R_f = 0.45$; TLC (hexane/EtOAc 4:1): $R_f = 0.20$; $[\alpha]_D^{20} = +59.9$ ($c = 1.0$, $CHCl_3$); ^{1}H NMR (200 MHz, $CDCl_3$): $\delta = 7.38-7.18$ (m, 30H), 5.52 (d, 1H, $J = 3.4$ Hz, H-1b), 5.39 (t, 1H, $J = 8.5$ Hz, H-4a), 5.35 (d, 1H, $J =$ 1.8 Hz, H-1c), 5.22 (dd, 1H, $J = 8.7$, 4.1 Hz, H-3a), 5.14 (dd, 1H, $J = 9.2$, 7.8 Hz, H-5a), 4.93 (d, 1H, $J = 11.3$ Hz), 4.86 (d, 1H, $J = 11.1$ Hz), 4.68–3.48 (m, 22H), 3.39 (dd, 1H, $J = 9.8$, 3.4 Hz), 2.08–0.88 (m, 25H), 2.06, 2.01 (2 s, 9H), 0.98, 0.89, 0.88 (3s, 3H each); ^{13}C NMR (50 MHz, $CDCl_3$): $\delta = 169.77$, 169.45, 169.35, 138.56, 138.39, 137.79, 128.41–126.98 (phenyl), 118.76, 100.41, 95.70, 79.72, 79.63, 76.80, 76.08, 75.96, 75.40, 74.78, 74.12, 73.36, 73.22, 72.78, 72.40, 72.04, 71.38, 70.98, 70.17, 69.42, 69.12, 68.73, 51.54, 47.95, 45.06, 44.41, 29.74, 26.87, 20.73, 20.65, 20.57, 20.26, 20.20, 17.03, 13.04, 9.54; elemental analysis calcd for $C_{76}H_{87}N_3O_{18}$: C 68.61, H 6.59, N 3.16; found: C 68.92, H 6.60, N 3.06.

***O*-(2,3,4,6-Tetra-*O*-benzyl-α-D-mannopyranosyl)-(1→4)-*O*-(2-azido-3,6-tri-*O*-benzyl-2-deoxy-β-D-glucopyranosyl)-(1→6)-3,4-5-tri-*O*-benzyl-1,2-*O*-(L-1,7,7-trimethyl[2.2.1]bicyclohept-6-ylidine)-D-*myo*-inositol** (**27**): To a stired solution of **26** (190 mg, 143 μmol) in methanol (25 mL) was added sodium methoxide (9 drops of a 0.5‰M solution in MeOH). After 4 h, the solution was neutralized with gaseous carbon dioxide, treated with 2 drops of Et_3N, concentrated, and coevaporated with toluene (2 × 10 mL). The residue was taken up in DMF (5 mL), next BnBr (155 μL, 1.30 mmol) and then 95 % NaH (93 mg, 3.66 mmol) was added portionwise with stirring. After 5 h, the reaction mixture was worked up as described for **23** (method

0947-6539/99/0501-0332 $ 17.50+.50/0 *Chem. Eur. J.* **1999**, *5*, No. 1

b). The obtained residue was purified by flash chromatography (hexane →hexane/EtOAc 6:1) to give **27** (190 mg, 90%) as a colorless syrup: TLC (hexane/EtOAc 4:1): $R_f = 0.45$: $[Ga]_D^{20} = +42.2$ ($c = 1.0$, $CHCl_3$); ^1H NMR (200 Mhz, $CDCl_3$): $\delta = 7.42-7.20$ (m, 45 H), 5.68 (d, 1 H, $J = 3.5$ Hz), 5.34 (d, 1 H, $J = 1.7$ Hz), 5.28–3.47 (m 35 H), 3.42 (dd, 1 H, $J = 9.9$, 3.5 Hz), 2.05–1.20 (m, 9 H), 1.12, 0.93, 0.89 (3 s, 3 H each); ^{13}C NMR (50 MHz, $CDCl_3$): $\delta = 138.82$, 138.54, 138.45, 138.36, 138.27, 138.06, 137.80, 128.50–126.93 (phenyl), 118.05, 100.81, 95.38, 80.81, 80.53, 79.79, 79.61, 77.97, 77.56, 76.82, 76.25, 76.02, 75.01, 74.79, 74.73, 74.65, 73.82, 73.27, 73.01, 72.92, 72.51, 72.19, 72.09, 70.05, 69.09, 68.37, 63.06, 51.55, 47.91, 45.07, 44.71, 29.79, 26.94, 20.56, 20.34, 9.66; MS FAB (thioglycerol matrix, NaI): *m/z*: 1497 ($[MNa]^+$).

***O*-(2-Azido-3,4,6-tri-*O*-benzyl-2-deoxy-α-D-glucopyranosyl) (1→4)-1,5,6-tri-*O*-benzyl-L-*myo*-inositol** (**28**): To a solution of **24** (240 mg, 230 μmol) in aqueous wetted $CHCl_3$ (4 mL) was added trifluoroacetic acid (0.5 mL) with stirring. After 6 h, the reaction mixture was concentrated and coevaporated with $CHCl_3$ (3×25 mL). The residue was purified by flash chromatography (hexane/EtOAc 6:5, 2.0×13.0 cm) to give **28** (175 mg, 84%) as a colorless syrup, which could be crystallized from Et_2O or Et_2O/hexane to give fine white needles: m.p. 131–132 °C; TLC (hexane/EtOAc 6:5): $R_f = 0.46$; $[\alpha]_D^{22} = +36.5$ ($c = 1.0$, $CHCl_3$); ^1H NMR (200 MHz, $CDCl_3$): $\delta = 7.39-7.08$ (m, 30 H), 5.39 (d, 1 H, $J = 3.6$ Hz), 5.08–4.65 (m, 9 H), 4.48 (d, 1 H, $J = 12.2$ Hz), 4.44 (d, 1 H, $J = 10.8$ Hz), 4.24–4.19 (m, 1 H), 4.13 (d, 1 H, $J = 12.2$ Hz), 4.08–3.88 (m, 4 H), 3.87 (d, 1 H, $J = 4.5$ Hz), 3.77 (t, 1 H, $J = 9.1$ Hz), 3.62 (ddd, 1 H, $J = 9.2$, 4.5, 2.8 Hz), 3.58 (dd, 1 H, $J = 10.2$, 3.6 Hz), 3.51 (dd, 1 H, $J = 9.6$, 2.7 Hz), 3.39 (t, 1 H, $J = 9.5$ Hz), 3.30 (dd, 1 H, $J = 11.0$, 2.2 Hz), 3.05 (dd, 1 H, $J = 11.0$, 1.5 Hz), 2.65 (s, 1 H); ^{13}C NMR (50 MHz, $CDCl_3$): $\delta = 138.41$, 138.36, 138.09, 137.75, 137.67, 128.51–127.28 (phenyl), 98.91, 81.65, 80.90, 80.76, 79.72, 77.93, 75.86, 75.43, 75.01, 74.71, 73.25, 72.68, 72.58, 71.04, 69.24, 67.27, 64.29; analysis calcd for $C_{54}H_{57}N_3O_{10}$: C 71.43, H 6.33, N 4.63; found: C 71.69, H 6.41, N 4.55.

***O*-(2,3,4,6-Tetra-*O*-benzyl-α-D-mannopyranosyl)-(1→4)-*O*-(2-azido-3,6-tri-*O*-benzyl-2-deoxy-α-D-glucopyranosyl)-(1→4)-1,5,6-tri-*O*-benzyl-L-*myo*-inositol** (**29**): To a solution of **27** (170 mg, 115 μmol) in aqueous wetted $CHCl_3$ (4 mL) was added trifluoroacetic acid (0.5 mL) with stirring. After 6 h, the reaction mixture was coevaporated with toluene (3×25 mL). The cloudy residue was purified by flash chromatography (hexane/EtOAc 7:5, 2.0×13.0 cm) to give **29** (136 mg, 88%) as a colorless syrup: TLC (hexane/EtOAc 7:5): $R_f = 0.32$; $[\alpha]_D^{20} = +40.5$ ($c = 1.0$, $CHCl_3$); ^1H NMR (300 MHz, $CDCl_3$): $\delta = 7.39-7.15$ (m, 45 H), 5.56 (d, 1 H, $J = 3.5$ Hz), 5.30 (d, 1 H, $J =$ 2.2 Hz), 4.99–4.26 (m, 18 H), 4.18 (bt, 1 H, $J = 2.5$ Hz), 4.10–3.99 (m, 4 H), 3.93–3.83 (m, 3 H), 3.76–3.47 (m, 10 H); ^{13}C NMR (50 MHz, $CDCl_3$): $\delta =$ 138.68, 138.44, 138.33, 138.29, 137.66, 137.56, 128.46–126.82 (phenyl), 100.53, 98.105, 81.47, 80.95, 80.47, 79.85, 79.69, 77.28, 76.10, 75.75, 75.07, 74.79, 74.68, 74.34, 73.28, 73.03, 72.94, 72.75, 72.61, 72.21, 72.01, 70.80, 69.54, 69.05, 68.52, 64.26; MS FAB (thioglycerol matrix, NaI): *m/z*: 1363 ($[M\mathrm{Na}]^+$).

1,2-Di-*O*-myristoyl-*sn*-glycero-3-yl dibenzylphosphite (**31**): To a stirred solution of 1,2-dimyristoyl-*sn*-glycerol[59] (450 mg, 877 μmol) and anhydrous tetrazole (246 mg, 3.51 mmol) in THF (12 mL) was slowly added dibenzyl *N,N*-diisopropylphosphoamidite (590 μL, 1.75 mmol). After 3 h, the reaction mixture was diluted with CH_2Cl_2.(100 mL) and successively washed with saturated $NaHCO_3$ solution, brine, and water (30 mL each). The organic layer was dried (Na_2SO_4), and the residue was subjected to flash chromatography (hexane/EtOAc 20:1 + 1% Et_3N) to give **31** (610 mg, 92%) as a colorless oil. To prevent oxidation, **31** was stored at −30 °C under an argon atmosphere. **31**: TLC (hexane/EtOAc 8:1 + 1% Et_3N): $R_f = 0.47$ with decomposition; $[\alpha]_D^{20} = +5.7$ ($c = 1.0$, $CHCl_3$); ^1H NMR (300 MHz, $CDCl_3$): $\delta = 7.36-7.29$ (m, 10 H), 5.21–5.14 (m, 1 H), 4.90–4.86 (m, 4 H), 4.31 (dd, 1 H, $J = 11.9$, 4.0 Hz), 4.14 (dd, 1 H, $J = 11.9$, 6.3 Hz), 4.05–3.89 (m, 2 H), 2.28 (t, 4 H, $J = 7.6$ Hz), 1.68–1.57 (m, 4 H), 1.27 (bs, 40 H), 0.89 (t, 6 H, $J = 7.6$ Hz); ^{13}C NMR (50 MHz, $CDCl_3$): $\delta = 173.30$, 172.94, 137.91, 128.84–127.31 (phenyl), 70.36, 70.27, 64.55, 64.33, 62.13, 60.82, 60.61, 34.23, 34.07, 31.91, 29.64, 29.47, 29.34, 29.27, 29.10, 24.86, 22.67, 14.10.

***O*-(2-Azido-3,4,6-tri-*O*-benzyl-2-deoxy-α-D-glucopyranosyl)-(1→6)-3,4,5-tri-*O*-benzyl-1-*O*-(1,2-di-*O*-myristoyl-*sn*-glycero-3-yl *R/S*-benzylphosphato)-D-*myo*-inositol** (**32**): A mixture of **28** (40.0 mg, 44.0 μmol), **31** (80.0 mg,106 μmol), and freshly activated, powdered 4 Å molecular sieves(30 mg) was added to CH_2Cl_2/pyridine (1 mL; 9:1) and stirred for 30 min at room temperature. Then, the mixture was cooled to −48 °C and treated with practical 95% pyridine hydrobromide perbromide (39 mg, 110 μmol). After stirring for 5 min, the reaction mixture was quenched with aqueous 10% $Na_2S_2O_3$ (1 mL), and allowed to warm to room temperature. Then, more aqueous 10% $Na_2S_2O_3$ (25 mL) was added and the solution was extracted with EtOAc (3×15 mL). The combined organic layers were washed with brine (20 mL), dried (Na_2SO_4), and evaporated. The residue was quickly chromatographed (hexane/EtOAc 3:1→2:1) to give **32** (37.2 mg, 54%; ds = 1.9:1 by ^1H NMR spectroscopy) as a colorless syrup, and unreacted **28** (11.0 mg, 28%). **32**: TLC (hexane/EtOAc 2:1): $R_f = 0.65$; $[\alpha]_D^{20} = +29.5$ ($c = 1.0$, $CHCl_3$); ^1H NMR (300 MHz, $CDCl_3$): $\delta = 7.41-7.03$ (m), 5.48(d, 1 H, J = 3.7Hz), 5.43 (d, 1 H, $J = 3.7$ Hz), 5.27–3.92 (m), 3.73–3.66 (m), 3.49 (dt, 1 H, $J = 9.9$, 2.8 Hz), 3.40 (dt, 1 H, $J = 9.3$, 1.9 Hz), 3.26–3.17 (m), 2.96 (d, 1 H, $J = 2.4$ Hz), 2.65 (d, 1 H, $J = 2.1$ Hz), 2.32–2.26 (m), 1.26 (bs), 0.89 (bt, $J = 7.0$ Hz); ^{13}C NMR (50 MHz, $CDCl_3$): $\delta = 173.28$, 173.16, 172.92, 172.80, 171.07, 138.36, 137.95, 137.83, 137.62, 128.75-127.42 (phenyl), 97.70, 97.49, 81.14, 80.39, 79.71, 79.60, 79.42, 78.16, 75.80, 75.47, 75.14, 74.70, 74.13, 73.96, 73.33, 72.62, 72.55, 70.36, 69.87, 69.76, 69.44, 69.24, 68.21, 67.67, 65.67, 63.05, 61.66, 60.33, 34.09, 33.98, 31.88, 29.63, 29.47, 29.32, 29.27, 29.10, 24.80, 22.65, 20.98, 14.16, 14.07; MS FAB (thioglycerol matrix, NaI): *m/z*: 1595 ($[M\mathrm{Na}]^+$).

***O*-(2,3,4,6-Tetra-*O*-benzyl-α-D-mannopyranosyl)-(1→4)-*O*-(2-azido-3,4,6-tri-*O*-benzyl-2-deoxy-α-D-glucopyranosyl)-(1→6)-3,4,5-tri-*O*-benzyl-1-*O*-(1,2-di-*O*-myristoyl-*sn*-glycero-3-yl *R/S*-benzylphosphato)-D-*myo*-inositol** (**33**): Compound **29** (60.0 mg, 44.7 μmol), **31** (71.0 mg, 93.8 μmol), and freshly activated, powdered 4 Å molecular sieves (30 mg) were added to CH_2Cl_2/pyridine (1 mL; 9:1). After stirring for 30 min at room temperature, the mixture was cooled to −44 °C and treated with practical 95% pyridine hydrobromide perbromide (35 mg, 98.7 μmol). After 5 min, the reaction mixture was worked up as described for **32**. The residue was immediately subjected to flash chromatography (hexane/EtOAc 3:1→1:1) to give **33** (25.0 mg, 28&%) as a colorless syrup {TLC (hexane/EtOAc 2:1): $R_f = 0.48$} and unreacted **29** (13.0 mg, 22%). Compound **33** decomposes rapidly and was therefore immediately subjected to the deprotection step (→2).

***O*-(2-Ammonio-2-deoxy-α-D-glucopyranosyl)-(1→6)-1-*O*-(1,2-di-*O*-myristoyl-*sn*-glycero-3-yl phosphate)-D-*myo*-inositol** (**1**): A mixture of **32** (18.4 mg, 11.7 μmol) and 10% Pd on charcoal (32 mg) in EtOAc/THF/EtOH/H_2O (5 mL; 2:1:1:1) was stirred in an atmosphere of H_2 (1 atm) at room temperature for 24 h. Then, the mixture was filtered through a pad of Celite, and the filter cake was washed with THF/EtOH/H_2O (1:1:1; $2 \times$ 3 mL). The filtrates were combined and evaporated in a vacuum centrifuge, to give **1** (10.7 mg, quant.) as a white solid: TLC (*n*BuOH/EtOH/30% aqueous NH_3/H_2O 2:2:1:3): $R_f = 0.72$; $[\alpha]_D^{20} = +59.0$ ($c = 0.38$, $CHCl_3$/MeOH/H_2O 1:1:0.3); MS FAB (thioglycerol/ PNB matrix, NaI): *m/z*: 960 ($[M+2\mathrm{Na}^+]$), 938 ($[M\mathrm{Na}^+]$); HRMS (thioglycerol/ TFA matrix) calcd for $C_{43}H_{82}NO_{17}P$: 916.53987, found 916.54040; elemental analysis Calcd for $C_{43}H_{82}NO_{17}P$: C 56.39, H 8.96, N 1.53; found: C 55.96, H 8.75, N 1.12.

***O*-α-D-Mannopyranosyl-(1→4)-*O*-(2-ammonio-2-deoxy-α-D-glucopyranosyl)-(1→6)-1-O-(1,2-di-*O*-myristoyl-*sn*-glycero-3-yl phospate)-D-*myo*-inositol** (**2**): A mixture of **33** (10.0 mg, 4.99 μmol) and 10% Pd on charcoal (42 mg) in EtOAc (1.8 mL), THF (1.2 mL), EtOH (1.2 mL), and H_2O (1.2 mL) was stirred in an atmosphere of H_2 (1 atm) at room temperature for 6 h, and worked up as described for **1**. The residue was chromatographed on silica gel {$CHCl_3$/MeOH/aqueous NH_3 (pH 8) 65:35:0.8; 1.5 × 8 cm} to give **2** (3.3 mg, 61%) as a colorless solid, that was lyophilized from dioxane/H_2O/*n*BuOH (2 mL; 10:5:1): TLC (*n*BuOH/EtOH/30% aqueous NH_3/H_2O 2:2:1:3): $R_f = 0.77$; $[\alpha]_D^{20} = +63.0$ ($c = 0.28$, $CHCl_3$/MeOH/H_2O 1:1:0.3); MS FAB (thioglycerol/PNB matrix, NaI): *m/z*: 1099 ($[M\mathrm{Na}^+]$); HRMS (thioglycerol/ TFA matrix) calcd for $C_{49}H_{92}NO_{22}P$: 1078.5927, found 1078.5949.

***O*-2-Ammonio-2-deoxy-α-D-glucopyranosyl-(1→6)-D-*myo*-inositol-1,2-cyclic phosphate** (**3**):[13b,29] Dichloromethyl phosphate (30.5 μL, 303 μmol) was added to pyridine (630 μL) with stirring. After 5 min, a white precipitate had formed, and after 30 min **27** (110 mg, 121 μmol) was added in one portion. This suspension was stirred for 2 h at room temperature and then quenched with saturated aqueous $NaHCO_3$ solution (1.25 mL). The reaction mixure was evaporated to dryness, taken up in water (10 mL), acidified with 2‰M aqueous HCl to pH 1 and immediately extracted with EtOAc (2×50 mL). The organic layers were combined, dried (Na_2SO_4) and concentrated to give a cloudy syrup which was immediately taken up in THF/EtOH/H_2O (1:1:1; 15 mL) containing NH_4OAc (38 mg, 493 μmol) and 10% Pd on charcoal (150 mg). This mixture was stirred under H_2

(1 atm) for 24 h. The resulting material was filtered through Celite, rinsed with ethanol and water. The filtrates were combined, concentrated, and loaded on a column of Dowex 1X4-200 resin (HCO_3^- form, 1.0 × 5.0 cm). Elution with an aqueous NH_4OAc gradient (0 → 0.2 M) and lyophilization afforded **3**[13b,29] (30 mg, 62%) as a colorless powder: TLC (IPrOH/30% aq NH_3/H2O 5:5:2): $R_f = 0.43$.

***O*-α-D-Mannopyranosyl-(1→4)-*O*-2-ammonio-2-deoxy-α-D-glucopyranosyl-(1→6)-D-*myo*-inositol-1,2-cyclic phosphate (4)**: Dichloromethyl phosphate (21.3 μL, 205 μmol) was added to pyridine (200 μl) with stirring. After 30 min, a solution of **29** (68 mg, 50.7 μmol) in pyridine (360 μL) was added dropwise. This suspension was stirred for 2 h at room temperature and then quenched with saturated aqueous $NaHCO_3$ solution (900 μL). After the evolution of gas had ceased, the reaction mixture was evaporated to dryness, and the residue was added to a solution of THF/EtOH/H_2O (1:1:1; 9 mL) containing NH_4OAc (25.4 mg, 329 μmol) and 10% Pd on charcoal (100 mg). This mixture was shaken under 45 psi H_2 in a Parr hydrogenator. After 20 h, more 10% Pd on charcoal (100 mg) was added and hydrogenating was continued for 48 h. Then, the resulting material was filtered through a pad of Celite with an aqueous wash. The filtrate was stirred with Sigma TMD-8 mixed bed resin (4 g) for 3 min, then filtered, and lyophilized to give **4** (25.8 mg, 90%) as a white solid: TLC (*i*PrOH/30% aqueous NH_3/H_2O 5:5:2): $R_f = 0.57$; $[\alpha]_D^{22} = +57.0$ ($c = 1.0$, H_2O); MS FAB (thioglycerol/ PNB matrix, NaI): m/z: 610 ($[M+2Na^+]$); HRMS (thioglycerol/ TFA matrix) calcd for $C_{18}H_{32}NO_{17}P$: 566.14861, found 566.14910.

X-ray structure determination: Data were collected at 250 K using an Oxford Cryostream device and the stated temperature was measured continuously during data collection. Semiempirical (ψ scan) absorption correction was applied. The strucure was solved by direct methods by using the SIR92 program.[60] The absolute configuration was not determined as it was known from synthesis and it was assigned according to the configurational angles.[37] The refinement was carried out by full-matrix least-squares procedures on F_{obs}. The hydrogen atoms obtained from difference Fourier synthesis were included in the refinement and their thermal factors were kept fixed during the last cycles of refinement. Most of the calculations were performed on a DEC3000-300X workstation using the XTAL3.4-system,[61] PESOS,[62] and PARST[63] programs. The atomic scattering factors were taken from the *International Tables for X-Ray Crystallography*, Vol. IV.[64] Crystal data: $C_{12}H_{12}NO_{12}P \cdot 5H_2O$, colorless prisms, crystal dimensions 0.50 × 0.30 × 0.17, space group orthorhombic, $P2_12_12_1$. The unit cell was determined by a least-squares fit from 37 reflections ($\theta < 45^\circ$); unit cell dimensions $a = 16.1045(11)$, $b = 12.3575(6)$, $c = 11.3828(4)$ Å, $V = 2066.3(2)$ Å^3, $Z = O17$, $\rho = 1.586$ g cm^{-3}, $M = 493.36$, $F(000) = 1048$, $\mu = 19.98$ cm^{-1}; four-circle diffractometer: Philips PW1100; bisecting geometry; graphite-oriented monochromator: $\omega/2\theta$ scans; detector apertures 1 × 1°, 1 min per reflection; $Cu_{K\alpha}$ radiation, scan width 1.5°, θ_{max} 65°. A total of 2018 independent reflections were collected, 1981 of which were observed ($2\sigma(I)$ criterion). Standard reflections:
2 reflections every 90 minutes showed no variation; max/min. transmission factors:
1.000/0.792; 377 variables, 1604 degrees of freedom, ratio of freedom 5.3, final shift/error 0.04. Empirical weighting scheme as to give no trends in $<\omega\Delta^2F$ vs. $<|F_{obs}|>$ and $<\sin\theta/\lambda>$; max. thermal value U22[O(20)] = 0.094(3) Å^2, final ΔF peaks −0.33/0.24 e Å^{-3}, final $R = 0.028$ and $Rw = 0.034$. Crystallographic data (excluding structure factors) for the structures reported in this paper have been deposited with the Cambridge Crystallographic Data Center as supplementary publication no. CCDC-100286. Copies of the data can be obtained free of charge on application to CCDC, 12 Union Road, Cambridge CB21EZ, UK (fax: (+44) 1223-336-033; e-mail: deposit@ccdc.cam.ac.uk).

NMR measurements: NMR experiments were recorded on Varian Unity 500 spectrometers, using about 3–5 mmolar solutions of the different compounds in D_2O, [D_6]DMSO or D_2O/SDS micelles. NOESY experiments were recorded using mixing times of 400, 600, and 800 ms. ROESY experiments used mixing times of 300 and 400 ms. In this case, the rf carrier frequency was set at $\delta = 6.0$, and the spin locking field was 2.5 KHz. Selective inversion 1D experiments were performed by using the DANTE-Z module.[65] In particular, 1D-NOESY, 1D-ROESY, and 1D-T-ROESY experiments were carried out. Additional experiments were performed by using the double pulse field gradient spin echo technique proposed by Shaka and co-workers.[66] NOESY experiments were recorded using mixing times of 600 and 800 ms. ROESY and T-ROESY experiments used mixing times of 300 and 400 ms. For T-ROESY the carrier was set at the residual water frequency and the spin locking field was 8.5 KHz. Under these conditions, $\sigma_{T\text{-}ROE}$ is the mean value of σ_{NOE} and σ_{ROE}.[67] The experiments were carried out at 299 K. Standard temperature control was used.

Molecular Modeling: Glycosidic torsion angles are defined as Φ H-1′-C-1′-O-1′-C-X, and Ψ C-1′-O-1′-C-X-H-X**.** Relaxed (Φ,Ψ) potential energy maps were calculated for **1** by using AMBER as modified by Homans and as integrated in Insight II and DISCOVER 94.0.[68] Only the *gg* and *gt* orientations of the lateral chain were used for the glucose and mannose moieties, since they have been shown to be rather more stable than the alternative *tg* conformers.[69] In addition, the three possible combinations of staggered conformers for the phosphate moiety were also considered. The starting position for the secondary hydroxyl groups was set as *r* (anticlockwise) or *c* (clockwise). In total, eighteen initial geometries were taken into account, and 18 different relaxed energy maps were built. In total, 7200 conformers were calculated for the acyclic-phosphate pseudo-disaccharide and 800 for the cyclic phosphate analogue. In all cases, the first step involved the generation of the corresponding rigid residue maps by using a grid step of 18°. Then, every Φ,Ψ point of this map was optimized by using 200 steepest descent steps, followed by 2500 conjugate gradient iterations. Following this protocol, the maximum rms derivative was smaller than 0.05 kcal mol^{-1} Å^{-1}. Despite the restriction set around the glycosidic linkages (4000 Kcal per rad^2), deviations smaller than 0.3° in Φ/Ψ values were observed in high energy regions. From these relaxed energy maps, adiabatic surfaces were built by choosing the lowest energy structure for a given Φ,Ψ point. Therefore in these surfaces, which represent a two-dimensional projection of a multidimensional hyperspace, points coexist which come from different geometries in terms of the secondary hydroxyl and hydroxymethyl groups.

Probability calculations: From the sixteen relaxed energy maps, calculated for each dielectric constant, the probability distribution was calculated for each Φ/Ψ point. Assuming that the entropy difference among the different conformers is negligible, the probability P of a given Φ/Ψ point is:[70] $P_{\Phi/\Psi} = \Sigma_i\{\exp(-E_i/RT)\}/\Sigma_i\Sigma_{\Phi\Psi}\{\exp(-E_{i\Phi,\Psi}/RT)\}$. This relationship can be used in a simple way to transform energy maps into probability maps. In our case, the sum of the numerator extends over sixteen points, which correspond to the sixteen relaxed maps. The sum on the denominator considers 7200 points, that is 18 maps consisting of 400 points each.

Molecular dynamics: Molecular dynamics simulations for the trisaccharide were performed by using the Amber/Homans force field. Two independent MD simulations were carried out. The initial structure of the trisaccharide was extensively minimized and then solvated with 233 water molecules in a cubic box of 20 Å, giving a density of about 1 g cm^{-3}. A cutoff of 9 Å was used for nonbonding interactions. Periodic boundary conditions and the minimum image model were employed. The simulations were performed at 300 K with 1 fs integration step. The equilibration period was 15 ps. After this period, structures were saved every 15 fs for the 400 ps simulation time. This short saving frequency was essential to get good correlation functions. In total, more than 25000 structures were collected for every simulation. MD trajectories were analyzed by using software written by ourselves. Overall reorientation was removed by diagonalizing the inertia tensor and subsequent superimposition of the principal inertia axis of every frame.[51] Then, internal correlation functions were calculated, and from these functions, generalized order parameters and internal correlation times were deduced, according to the Lipari and Szabo model-free approach. In addition, average distances between intraresidue and inter-residue proton pairs were calculated from the dynamics simulations.

NOE calculations: The first step in the NOE calculations was to estimate the interproton average distances, using a $<r^{-6}>_{kl}$ average. The estimated probability distributions from the relaxed energy maps were used to calculate the average distances according to Equation (a).

$$<r^{-6}>_{kl} = \Sigma P_{(\Phi\Psi)} * r^{-6}_{kl(\Phi\Psi)} \quad \text{(a)}$$

In addition, the average distances were also estimated from the MD simulations, considering the interproton distance for every saved frame [Eq. (b)], where n represents the total number of frames.

$$<r^{-6}>_{kl} = \Sigma(1/n) * r^{-6}_{kl(\Phi\Psi)} \quad \text{(b)}$$

0947-6539/99/0501-0334 $ 17.50+.50/0 *Chem. Eur. J.* **1999**, *5*, No. 1

The steady state 1D-NOE and the transient 1D and 2D-NOESY and ROESY spectra were calculated according to the complete relaxation matrix method assuming isotropic motion, external relaxation of 0.1 s^{-1}, and different overall correlation times, τ_c. All the spectra were simulated from the average relaxation rates (from $< r^{-6} >_{kl}$) calculated from both the relaxed relative energies and the MD trajectories at 300 K. In the case of the steady-state NOEs, the calculations were performed by solving the simultaneous set of linear equations proposed by Noggle and Schrimer,[71] while the NOESY and ROESY spectra were simulated using the protocol outlined by Cagas and Bush.[72] All the NOE calculations were performed by using software written by out ourselves. The software is available from the authors.

Biological assays: Preparation of explant cultures and measurement of cell proliferation: Experiments were carried out on chicken embryo otic vesicles, corresponding to stage 18.[73] Otic vesicles were isolated and grown in culture as previously described.[74] The standard culture medium consisted of serum-free M199 medium with Earle's salts supplemented with 20 mM glutamine (Seromed), 25 mM HEPES (Sigma) and antibiotics (penicillin, 50 UI mL^{-1} and streptomycin, 50 mg mL^{-1}) (Seromed). Foetal bovine serum was purchased from Flow. Incubations were carried out at 37 °C in a water-saturated atmosphere containing 5 % CO_2. Compound **3** was added to the basic medium at concentrations ranging between 0.1 – 100 μM as indicated in the text. Insulin-like growth factor-I was purchased from Boehringer Mannheim. Otic vesicles were made quiescent by incubation in the absence of serum for 24 h prior to stimulation. Cell proliferation was estimated by scintillation counting of the incorporated [^{3}H]thymidine (46 Ci $mmol^{-1}$, Amersham) into trichloroacetic acid precipitated explants.[74]

Antisense oligonucleotides: In some experiments, 15 base-pair oligonucleotides were added to the culture medium. Phosphorothioate (S-) modified oligonucleotides (Oligos Etc) were used.[32] Antisense oligonucleotides were directed against the ATG initiation codon of the chicken c-*fos* gene[75] and the sequence was 5′-GCCCTGGTACATCAT-3′. The sequence of the sense oligomer was 5′-ATGATGTACCAGGGC-3′. A random oligonucleotide containing the same base composition of the antisense oligonucleotide but with a random sequence was: 5′-CCCCCGGGTTTTAAA-3′.

Immunoblotting: Otic vesicle explants were homogenized in SDS-PAGE sample buffer with 1 mM phenylmethylsulfonyl fluoride and then frozen immediately. Gels were loaded with solutions containing equal amounts of proteins, typically two otic vesicles per condition.[32] Proteins were resolved on 9 % polyacrylamide gels[76] and then transferred to PVDF membranes (Dupont-NEN). Filters were blocked with TRIS-buffered saline with added 5 % (wt/vol) nonfat dried milk and incubated with an anti-Fos sheep polyclonal antibody (Cambridge Research Biochem) diluted 1/2000. Filters were subsequently washed and incubated with a rabbit anti-sheep immunoglobulin conjugated with peroxidase (Calbiochem) diluted 1/1000. Bound peroxide activity was visualized by chemiluminescence (Dupont-NEN) and quantified by densitometry.

Acknowledgements

Thanks are given to DGICYT (Spain) for financial support (grants no. PB93-0127-C02-01, PB93-0125H and PB93-0098). H. D. is grateful to the Deutsche Forschungsgemeinschaft (DFG) and the European Union (HCM Programme; CARENET-1 Network) for a postdoctoral fellowships. J.-F. E. thanks M.E.C. for a FPU Fellowship. Y. L. is supported by a MEC-CSIC contract.

[1] *Phospholipid Metabolism in Cellular Signalling* (Ed.: J. M. Mato), CRC Press, Boca Raton, **1990**.
[2] N. Divecha, R. F. Irvine, *Cell* **1995**, *80*, 269 – 278.
[3] E. Kilgour, *Cell Signal* **1993**, *5*, 97 – 105.
[4] G. N. Gaulton, J. C. Pratt, *Seminars in Immunology* **1994**, *6*, 97 – 104.
[5] T. W. Rademacher, H. Caro, S. Kunjara, D. Y. Wang, A. L. Greenbaum, P. MacLean, *Braz. J. Med. Biol. Res.* **1994**, *27*, 327 – 341.
[6] J. M. Mato, *Cell Signal* **1989**, *1,* 143-146.
[7] G. Romero, J. Larner, *Advan. Pharmacol*. **1993**, *24*, 21 – 50.
[8] A. R. Saltiel, *FASEB J.* **1994** *8*, 1034 – 1040.
[9] J. M. Mato, K. Kelly, A. Abler, L. Jarrett, B. E. Corkey, B. E. Cashel, D. Zopf, *Biochem. Biophys. Res. Commun*. **1988**, *146*, 764 – 770.
[10] J. Larner, L. C. Huang, C. F. W. Schwartz, A. S. Oswald, T. Y. Shen, M. Kinter, G. Tang, K. Zeller, *Biochem. Biophys. Res. Commun*. **1988**, *155*, 1416 – 1426.
[11] D. R. Jones, M. A. Avila, C. Sanz, I. Varela-Nieto, *Biochem. Biophys. Res. Commun*. **1997**, *233*, 432 – 437.
[12] H. N. Caro, A. Guadaño, M. Bernabé, M. Martín-Lomas, J. M. Mato, R. A. Dwek, T. W. Rademacher, *Glycoconjugate J.* **1993,** *10*, 242.
[13] a) A. Zapata, M. Martín-Lomas, *Carbohydr. Res.* **1992**, *234*, 93 – 106; b) A. Zapata, Y. León, J. M. Mato, I. Varela-Nieto, S. Penadés, M. Martín-Lomas, *Carbohydr. Res.* **1994**, *264*, 21 – 31; c) C. Jaramillo, J. L. Chiara, M. Martín-Lomas, *J. Org. Chem*. **1994**, *264*, 3135 – 3141; d) N. Khiar, M. Martín-Lomas, *J. Org. Chem*. **1995**, *60*, 7017 – 7021.
[14] For a recent review on the synthesis of glycosylphosphatidylinositol anchors, including former preparations of some of the structures presented in this paper, see: R. Gigg, J. Gigg in *Glycopeptides and Related Compounds* (Eds.: D. G. Large, C. D. Warren), Marcel Dekker, New York, **1997**, pp. 327 – 392.
[15] a) I. Varela-Nieto, J. Represa, M. A. Avila, C. Miner, J. M. Mato, F. Giraldez, *Dev. Biol*. **1991**, *143*, 432 – 435; b) J. Represa, M. A. Avila, C. Miner, F. Giraldez, G. Romero, R. Clemente, J. M. Mato, I. Varela-Nieto, *Proc. Natl. Acad. Sci. USA* **1991**, *88*, 8016 – 8019; c) V. Basta, P. Bruni, R. Clemente, F. Vanini, P. Ochoa, G. Romero, M. Fernararo, I. Varela-Nieto, *Exp. Cell Res.* **1992**, *200*, 439 – 443.
[16] R. R. Schmidt, W. Kinzi, *Adv. Carbohydr. Chem. Biochem.* **1994**, *50*, 21 – 123.
[17] J. Banoub, P. Boulanger, D. Lafont, *Chem. Rev*. **1992**, *92*, 1167 – 1195.
[18] G. Grundler, R. R. Schmidt, *Liebigs Ann. Chem*. **1984**, 1826 – 1847.
[19] A. Vasella, C. Witzig, J. L. Chiara, M. Martín-Lomas, *Helv. Chim. Acta* **1991**, *74,* 2073 – 2077.
[20] G. Excoffier, D. Gagnaire, P. Utille, *Carbohydr. Res.* **1975**, *39*. 368 – 373.
[21] W. Kinzy, R. R. Schmidt, *Liebigs Ann. Chem.* **1985**, 1537 – 1545.
[22] M. Flores, J. L. Chiara, M. Martín-Lomas, unpublished results.
[23] a) R. D. Groneberg, T. Miyazaki, N. A. Stylianides, T. J. Schulze, W. Stahl, E. P. Schreiner, T. Suzuki, Y. Iwabuchi, A. L. Smith, K. C. Nicolaou, *J. Am. Chem. Soc.* **1993**, *115*, 7593 – 7611; b) M. S. Motawia, J. Marcussen, B. L. Moeller, *J. Carbohydr. Chem.* **1995**, *14*, 1279 – 1294.
[24] R. R. Schmidt, J. Michel, M. Roos, *Liebigs Ann Chem.* **1984**, 1343 – 1357.
[25] a) Y. Watanabe, M. Tomioka, S. Ozaki, *Tetrahedron* **1995**, *51*, 8969 – 8976; b) Y. Watanabe, T. Yamamoto, S. Ozaki, *J. Org. Chem*. **1996,** *61*, 14 – 15.
[26] a) K. S. Bruzic, G. M. Salamoczyk, *Carbohydr. Res.* **1989**, *195*, 67 – 73; b) K. M. Pietrusiewicz, G. M. Salamonczyk, G. M: Bruzic, W. Wieczorec, *Tetrahedron* **1992**, *48*, 5523 – 5542.
[27] K. S. Bruzic, M. D. Tsai, *J. Am. Chem. Soc.* **1992**, *114*, 6361 – 6374.
[28] J. Smrt, J. Catlin, *Tetrahedron Lett*. **1970**, *58,* 5081 – 5082.
[29] R. Plourde, M. d'Alarcao, A. R. Saltiel, *J. Org. Chem*. **1992**, *57*, 2606 – 2610.
[30] Y. Watanabe, E. Inada, M. Jinno, S. Ozaki, *Tetrahedron Lett*. **1993**, *34*, 497 – 500.
[31] K. L. Yu, B. Fraser-Reid, *Tetrahedron Lett.* **1988**, *29*, 979 – 982.
[32] Y. León, C. Miner, L. Ariza-McNaughton, J. J. Represa, F. Giraldez, *Dev. Biol*. **1995,** *167*, 75 – 86.
[33] J. J. Represa, A. Sánchez, C. Miner, J. Lewis, F. Giraldez, *Development* **1990**, *110*, 1081 – 1090.
[34] Y. León, C. Sanz, F. Giraldez, J. M. Mato, J. Represa, Y. Varela-Nieto, *Endocrinology* **1995**, *136*, 3494 – 3503.
[35] F. Allen, J. E. Davis, J. J. Galloy, O. Johnson, O. Kennard, C. F. Macrae, E. M. Mitchell, J. M. Smith, D. G. Watson, *J. Chem. Info. Compt. Sci*. **1991**, *31*, 187 – 204
[36] D. Cremer, J. A. Pople, *J. Am. Chem. Soc*. **1975**, *97*,1354 – 1358
[37] F. H. Cano, C. Foces-Foces, J. Jimenez-Barbero, M. Bernabé, M. Martín-Lomas, S. Penadés, *Tetrahedron* **1985**, *41*, 3875 – 3886.
[38] a) C. T. Weller, M. McConville, S. W. Homans, *Biopolymers* **1994**,*34*, 1155 – 1163; b) S. W. Homans, A. Mehlert, S. J. Turco, *Biochemistry* **1992**, *31*, 654 – 661.
[39] A. D. French, J. W. Brady, *ACS Symp. Ser.* **1990**,*430*.

[40] R. U. Lemieux, S. Koto, D. Voisin, *ACS Symp. Ser.* **1979**, *87*, 17 – 29.
[41] R. Woods, *Curr. Opin. Struct. Biol.* **1995**, *5*, 666 – 671.
[42] S. J. Weiner, P. A. Kollman, D. A. Case, U. C. Singh, C. Ghio, *J. Am. Chem. Soc.* **1984**, *106*, 765 – 784.
[43] S. W. Homans, A. *Biochemistry* **1990**,*29*, 9110 – 9118.
[44] T. Peters, B. M. Pinto, *Curr. Opin. Struct. Biol.* **1996**, *6*, 710 – 720.
[45] J. Dabrowski, T. Kozar, H. Grosskurth, N. E. Nifant'ev, *J. Am. Chem. Soc.* **1995**, *117*, 5534 – 5539.
[46] D. Neuhaus, M. P. Williamson, *The Nuclear Overhauser Effect in Structural and Conformational Analysis*, **1989**, VCH, New York.
[47] J. M. Coteron, K. Singh, J. L. Asensio, M. Dominguez-Dalda, A. Fernandez-Mayoralas, J. Jimenez-Barbero, M. Martín-Lomas, *J. Org. Chem.* **1995**, *60*, 1502 – 1519.
[48] J. W. Brady, R. K. Schmidt, *J. Phys. Chem.*, **1993**, *97*, 958 – 966.
[49] P. J. Hajduk, D. A. Horita, L. E. Lerner, *J. Am. Chem. Soc.* **1993**, *115*, 9196 – 9201.
[50] M. Philippopoulos, C. Lim, *J. Phys. Chem* **1994**, *98*, 8264 – 8273.
[51] R. Bruschweiler, B. Roux, M. Blackledge, C. Griesinger, M. Karplus, R. R. Ernst, *J. Am. Chem. Soc.* **1992**, *114,* 2289 – 2302.
[52] G. Lipari, A. Szabo, *J. Am. Chem. Soc.* **1982**, *104,* 4546 – 4559.
[53] A. Poveda, J. L. Asensio, M. Martín-Pastor, J. Jimenez-Barbero, *Chem. Comm.* **1996**, 421 – 422.
[54] A. Poveda, J. L. Asensio, M. Martín-Pastor, J. Jimenez-Barbero, *Carbohydr. Res.* **1997**,*300*, 3 – 10.
[55] L. R. Brown, B. T. Farmer, *Methods Enzymol.* **1989**, *176*, 199 – 216.
[56] L. Poppe, H. van Halbeek, D. Acquoti, S. Sonnino, *Biophys. J.* **1994**, *66*, 1642 – 1652.
[57] L. Emsley, *Methods Enzymol.* **1994**, *239*, 207 – 246.
[58] K. B. Wiberg, W. C. Cunningham Jr., *J. Org. Chem.* **1990**, *55*, 679 – 684.
[59] E. Eibl, J. O. McIntyre, E. A. M. Fleer, S. Fleischer, *Methods Enzymol.* **1983**, *98*, 623 – 632.
[60] A. Altomare, M. C. Burla, M. Camalli, G. Cascarano, C. Giacovazzo, A. Guagliardi, G. Polidori, *J. Appl. Crystallogr.* **1994**, 435.
[61] S. R. Hall, C. S. D. King, J. M. Stewart, Xtal3.4, Ed. University of Western Australia, Perth, **1995**.
[62] M. Martinez-Ripoll, F. H. Cano, **1975**, unpublished program.
[63] M. Nardelli, *Comput. Chem.* **1983**, *7*, 95 – 98.
[64] *International Tables for X-Ray Crystallography*, *Vol. IV*, Kynoch Press, Birmingham, **1974**.
[65] C. Roumestand, J. Mispleter, C. Austry, D. Canet, *J. Magn. Res. B* **1995**, *109*, 153 – 163.
[66] K. Stott, J. Stonehouse, J. Keeler, T. L. Hwang, A. J. Shaka, *J. Am. Chem. Soc.* **1995**, 117, 4199 – 4200.
[67] T. L. Hwang, A. J. Shaka, *J. Am. Chem. Soc.* **1992**, *114*, 3157 – 3158.
[68] Insight II/Discover 94.0, Biosym Technol., San Diego, CA, USA.
[69] K. Bock, J. O. Duus, *J. Carbohydr. Chem.* **1994** , *13*, 513 – 543.
[70] D. A. Cumming, J. P. Carver, *Biochemistry* **1995**, *26*, 6664 – 6676.
[71] J. H. Noggl, R. E. Schrimer, *The nuclear Overhauser effect: Chemical Applications*, Academic Press, New York, **1971**.
[72] P. Cagas, C. A. Bush, *Biopolymers.* **1990**, *30*, 1123 – 1138.
[73] V. Hamburger, H. L. Hamilton, *J. Morphol.* **1951**, *88*, 49 – 92.
[74] J. Represa, C. Miner, F. Giraldez, *Development* **1988**, *102*, 87 – 91.
[75] K. T. Fujiwara, K. Ashida, H. Nishina, H. Iba, N. J. Miyajima, M. Nishizawa, S. Kawai, *J. Virol.* **1987**, *61*, 4012 – 4018.
[76] U. K. Laemmli, *Nature* **1970**, *227*, 680 – 685.

Received: February 18, 1998
Revised version: August 31, 1998 [F1012]